Rapporter och meddelanden 141

Geology of the Northern Norrbotten ore province, northern Sweden

Paper 9 (13)

Editor: Stefan Bergman

SGU
Sveriges geologiska undersökning
Geological Survey of Sweden

Rapporter och meddelanden 141

Geology of the Northern Norrbotten ore province, northern Sweden

Editor: Stefan Bergman

Sveriges geologiska undersökning
2018

ISSN 0349-2176
ISBN 978-91-7403-393-9

Cover photos:
Upper left: View of Torneälven, looking north from Sakkaravaara, northeast of Kiruna. ***Photographer:*** Stefan Bergman.
Upper right: View (looking north-northwest) of the open pit at the Aitik Cu-Au-Ag mine, close to Gällivare. The Nautanen area is seen in the background. ***Photographer:*** Edward Lynch.
Lower left: Iron oxide-apatite mineralisation occurring close to the Malmberget Fe-mine. ***Photographer:*** Edward Lynch.
Lower right: View towards the town of Kiruna and Mt. Luossavaara, standing on the footwall of the Kiruna apatite iron ore on Mt. Kiirunavaara, looking north. ***Photographer:*** Stefan Bergman.

Head of department, Mineral Resources: Kaj Lax
Editor: Stefan Bergman

Layout: Tone Gellerstedt och Johan Sporrong, SGU
Print: Elanders Sverige AB

Geological Survey of Sweden
Box 670, 751 28 Uppsala
phone: 018-17 90 00
fax: 018-17 92 10
e-mail: sgu@sgu.se
www.sgu.se

Table of Contents

Introduktion

Stefan Bergman & Ildikó Antal Lundin

Den här rapporten presenterar de samlade resultaten från ett delprojekt inom det omfattande tvärvetenskapliga Barentsprojektet i norra Sverige. Projektet initierades av Sveriges geologiska undersökning (SGU) som ett första led i den svenska mineralstrategin. SGU fick ytterligare medel av Näringsdepartementet för att under en fyraårsperiod (2012–2015) samla in nya geologiska, geofysiska och geokemiska data samt för att förbättra de geologiska kunskaperna om Sveriges nordligaste län. Det statligt ägda gruvbolaget LKAB bidrog också till finansieringen. Projektets strategiska mål var att, genom att tillhandahålla uppdaterad och utförlig geovetenskaplig information, stödja prospekterings- och gruvindustrin för att förbättra Sveriges konkurrenskraft inom mineralnäringen. Ny och allmänt tillgänglig geovetenskaplig information från den aktuella regionen kan hjälpa prospekterings- och gruvföretag att minska sina risker och prospekteringskostnader och främjar därigenom ekonomisk utveckling. Dessutom bidrar utökad geologisk kunskap till en effektiv, miljövänlig och långsiktigt hållbar resursanvändning. All data som har samlats in i projektet lagras i SGUs databaser och är tillgängliga via SGU.

Syftet med det här delprojektet var att få en djupare förståelse för den stratigrafiska uppbyggnaden och utvecklingen av de mineraliserade ytbergarterna i nordligaste Sverige. Resultaten, som är en kombination av ny geologisk kunskap och stora mängder nya data, kommer att gynna prospekterings- och gruvindustrin i regionen i många år framöver.

Norra Norrbottens malmprovins står för en stor del av Sveriges järn- och kopparmalmsproduktion. Här finns fyra aktiva metallgruvor (mars 2018) och mer än 500 dokumenterade mineraliseringar. Fyndigheterna är av många olika slag, där de viktigaste typerna är stratiforma kopparmineraliseringar, järnformationer, apatitjärnmalm av Kirunatyp och epigenetiska koppar-guldmineraliseringar. En vanlig egenskap hos de flesta malmer och mineraliseringar i Norr- och Västerbotten är att de har paleoproterozoiska vulkaniska och sedimentära bergarter som värdbergart. För undersökningarna valdes ett antal nyckelområden med bästa tillgängliga blottningsgrad. De utvalda områdena representerar tillsammans en nästan komplett stratigrafi i ytbergarter inom åldersintervallet 2,5–1,8 miljarder år.

Rapporten består av tretton kapitel och inleds med en översikt över de geologiska förhållandena, som beskriver huvuddragen i de senaste resultaten. Översikten följs av fyra kapitel (2–5) som huvudsakligen handlar om litostratigrafi och åldersbestämningar av ytbergarterna. Huvudämnet för de därpå följande fem kapitlen (6–10) är 3D-geometri och strukturell utveckling. Därefter kommer två kapitel (11–12) som fokuserar på U-Pb-datering av en metamorf respektive intrusiv händelse. Rapporten avslutas med en studie av geokemin hos morän i Norra Norrbottens malmprovins (kapitel 13).

Introduction

Stefan Bergman & Ildikó Antal Lundin

This volume reports the results from a subproject within the Barents Project, a major programme in northern Sweden. The multidisciplinary Barents Project was initiated by SGU as the first step in implementing the Swedish National Mineral Strategy. SGU obtained additional funding from the Ministry of Enterprise and Innovation to gather new geological, geophysical and till geochemistry data, and generally enhance geological knowledge of northern Sweden over a four-year period (2012–2015). The state-owned iron mining company LKAB also helped to fund the project. The strategic goal of the project was to support the exploration and mining industry, so as to improve Sweden's competitiveness in the mineral industry by providing modern geoscientific information. Geological knowledge facilitates sustainable, efficient and environmentally friendly use of resources. New publicly available geoscientific information from this region will help exploration and mining companies to reduce their risks and exploration costs, thus promoting economic development. All data collected within the project are stored in databases and are available at SGU.

This subproject within the Barents Project aims to provide a deeper understanding of the stratigraphy and depositional evolution of mineralised supracrustal sequences in northernmost Sweden. The combined results in the form of new geological knowledge and plentiful new data will benefit the exploration and mining industry in the region for many years to come.

The Northern Norrbotten ore province is a major supplier of iron and copper ore in Sweden. There are four active metal mines (March 2018) and more than 500 documented mineralisations. A wide range of deposits occur, the most important types being stratiform copper deposits, iron formations, Kiruna-type apatite iron ores and epigenetic copper-gold deposits. A common feature of most deposits is that they are hosted by Palaeoproterozoic metavolcanic or metasedimentary rocks. A number of key areas were selected across parts of the supracrustal sequences with the best available exposure. The areas selected combine to represent an almost complete stratigraphic sequence.

This volume starts with a brief overview of the geological setting, outlining some of the main recent achievements. This is followed by four papers (2–5) dealing mainly with lithostratigraphy and age constraints on the supracrustal sequences. 3D geometry and structural evolution are the main topics of the next set of five papers (6–10). The following two contributions (11–12) focus on U-Pb dating of a metamorphic event and an intrusive event, respectively. The volume concludes with a study of the geochemical signature of till in the Northern Norrbotten ore province (13).

Authors, paper 9:
Johan Jönberger
Geological Survey of Sweden
Department of Mineral Resources,
Uppsala, Sweden

Cecilia Jönsson
Geological Survey of Sweden
Department of Mineral Resources,
Uppsala, Sweden

Stefan Luth
Geological Survey of Sweden
Department of Mineral Resources,
Uppsala, Sweden

9. Geophysical 2D and 3D modelling in the areas around Nunasvaara and Masugnsbyn, northern Sweden

Johan Jönberger, Cecilia Jönsson & Stefan Luth

ABSTRACT

This chapter focuses on the geophysical aspects of two key areas in northern Sweden with the emphasis on modelling the subsurface conditions primarily using magnetic and gravity data. The areas dealt with here are Nunasvaara, located 10 km west of the village of Vittangi, and Masugnsbyn, located 60 km northwest of Pajala. The areas surrounding both Nunasvaara and Masugnsbyn are well covered by pre-existing magnetic, electromagnetic and gravity geophysical data. Moreover, there is good coverage of petrophysical samples that have been analysed for density and magnetic properties. Using these data sets together with newly acquired geophysical and petrophysical information, 2D and 3D models have been constructed for a number of strategic locations to provide more information about subsurface conditions and ore-bearing lithologies. In Nunasvaara two 2D geophysical models, based on ground magnetic, gravity and petrophysical information, have been made across the greenstones. One profile is regional with a length of 11 km, whereas the other is a relatively short 2 km profile. An inversion model based on VLF data has been generated along the shorter profile, which crossed several known graphite-bearing black schist horizons. The modelling results show consistently east-dipping geometries in the northeastern part of Nunasvaara, while the regional model shows mostly vertical or west-dipping structures. The regional model suggests that the greenstones in the central part have a dome-shaped structure, surrounding an area with local magnetic and gravity minima. In the area around Masugnsbyn 3D models of the Masugnsbyn iron ore deposit have been made, based on dense gravity data and correlated to borehole information. The model shows a width between 50 and 150 m of the mineralised skarn, represented by a vertical slab (central model). This correlates well with the ore zone presented in Witschard et al. (1972). A forward 3D regional model over a large part of the area, based primarily on airborne magnetic data and petrophysical information, was also constructed. Newly acquired geophysical data have also provided important input to improve interpretation of the lithological and stratigraphic relationships along this regional profile. This new model gives new insight into the geometries of the volcanic rocks in the western part of the profile. It was found that these rocks dip to the east, unlike the older profile from Padget (1970), which shows west-dipping structures.

NUNASVAARA

Geological introduction

The bedrock in the Nunasvaara area consists predominantly of metavolcanic and metavolcaniclastic rocks of basaltic to andesitic composition, metasedimentary rocks including graphite-bearing black schist, and metadolerites (Fig. 1). These rocks are part of the *Vittangi greenstone group (VGG)*, which has a lateral extent of approximately 9 × 11 km extending N–NE (Eriksson & Hallgren 1975). The VGG in this area is surrounded by intrusions ranging from gabbro to granite belonging to the *Haparanda, Perthite monzonite* and *Lina* suites. Several mineralisations occur, including skarn iron and graphite deposits. For a more detailed description of the geology and lithostratigraphy around Nunasvaara, the reader is referred to Lynch et al. (2018).

Geophysical interpretation in the Nunasvaara area

A considerable amount of geophysical information is available for the Nunasvaara area. Airborne surveys have been conducted by SGU and LKAB on several occasions on which different geophysical data sets have been acquired, including magnetic, radiometric and electromagnetic data (slingram and VLF). In addition, dense ground magnetic, slingram and gravity measurements have been made over the entire area, together with extensive sampling for petrophysical analysis. More information about these previous geophysical investigations can be found in Lynch & Jönberger (2013).

The overall pattern of the magnetic and gravity field, along with the electromagnetic map (slingram data) represents lithological units in the area. The bedrock mainly consists of basaltic to andesitic metavolcanic rocks (tuffs) and metadolerites. The magnetic properties vary considerably, reflected in the statistics on the petrophysical samples in Figure 2 and Table 1. These variations can be seen on the magnetic anomaly map (Fig. 3) of the western part of the area, where tuffs generate both a banded pattern of relatively narrow, high-magnetic anomalies along with areas of considerably lower magnetic signature. Sequences of skarn iron ores, mainly in the west of the area, cause the strongest anomalies

Table 1. Tabular presentation of the petrophysical properties in the area, subdivided into the main lithologies.

Rock type	No. of samples	Density (SI), mean	Density (SI) Std. dev.	Susceptibility x 10^{-5} (SI) min	Susceptibility x 10^{-5} (SI) max	Susceptibility x 10^{-5} (SI) median	Q-value min	Q-value max	Q-value median
Basalt-andesite	205	2 958	117	9	44 850	165	0.03	94.77	0.54
Granite	31	2 632	30	6	4 315	902	0.01	1.06	0.13
Gabbro-diorite	54	2 954	95	7	49 730	4 501	0.05	29.00	0.29
Dolerite	118	2 979	93	13	117 200	279	0.02	37.42	0.79
Carbonate	8	2 779	74	16	1 074	38	0.09	4.26	0.35
Schist	22	2 765	134	-22	1 910	82	-0.87	180.62	0.83
Skarn	7	3 597	225	834	408 500	214 900	1.79	37.55	6.59

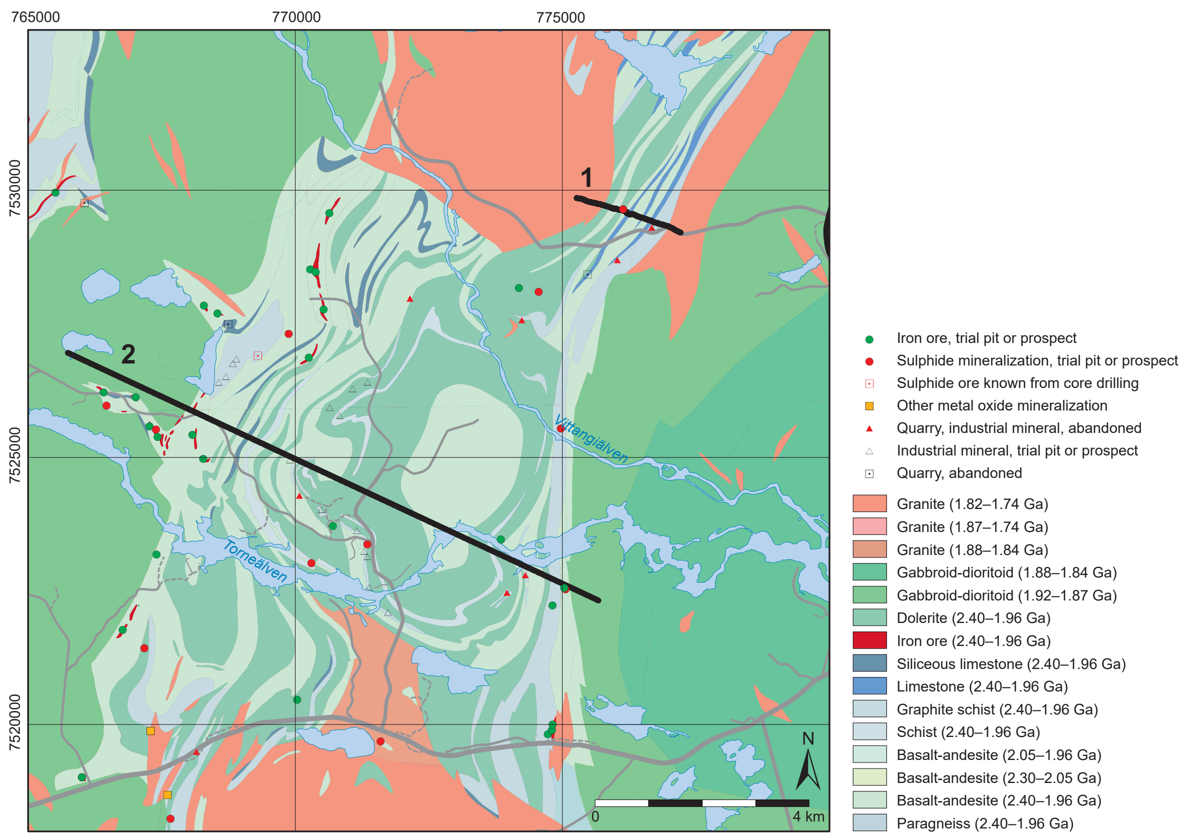

Figure 1. Bedrock map of the area around Nunasvaara (after Bergman et al. 2012). The mineralisation occurrences are shown on the map. Black lines represent the extent of profiles that have been modelled using geophysical data.

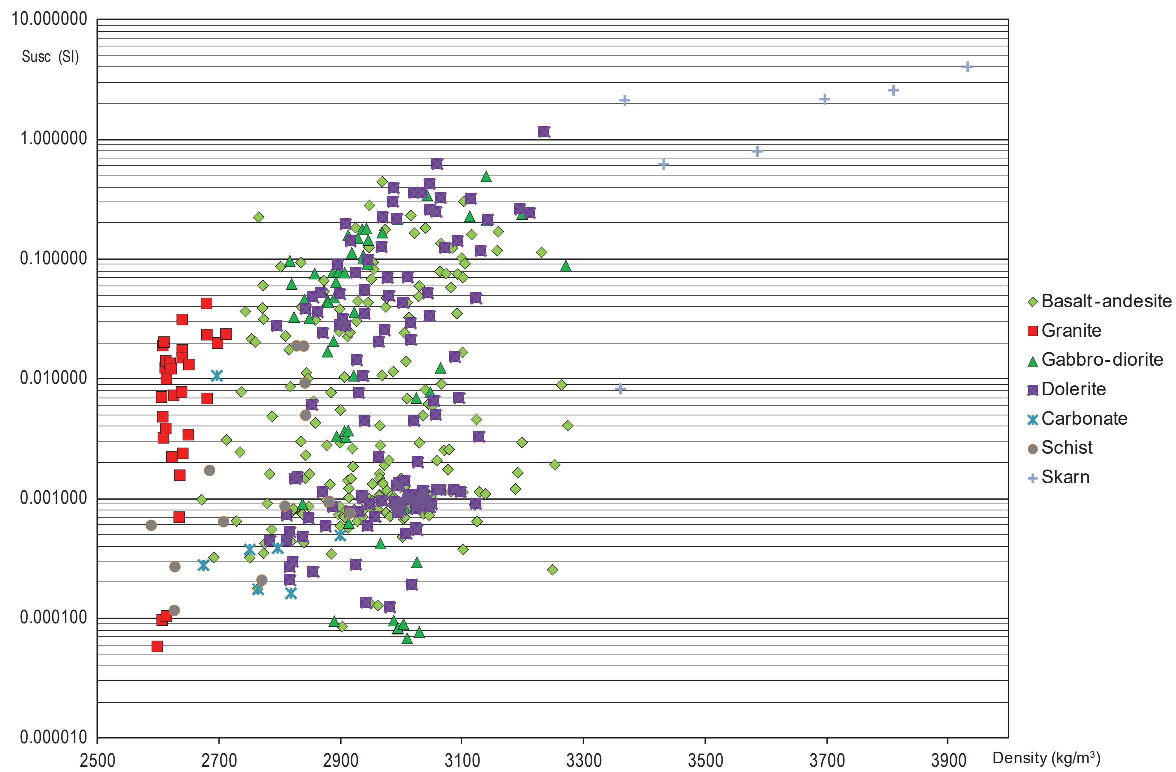

Figure 2. Petrophysical properties of the different lithologies in the area. Magnetic susceptibility (SI unit) v density (kg/m³). The total number of petrophysical samples is 445.

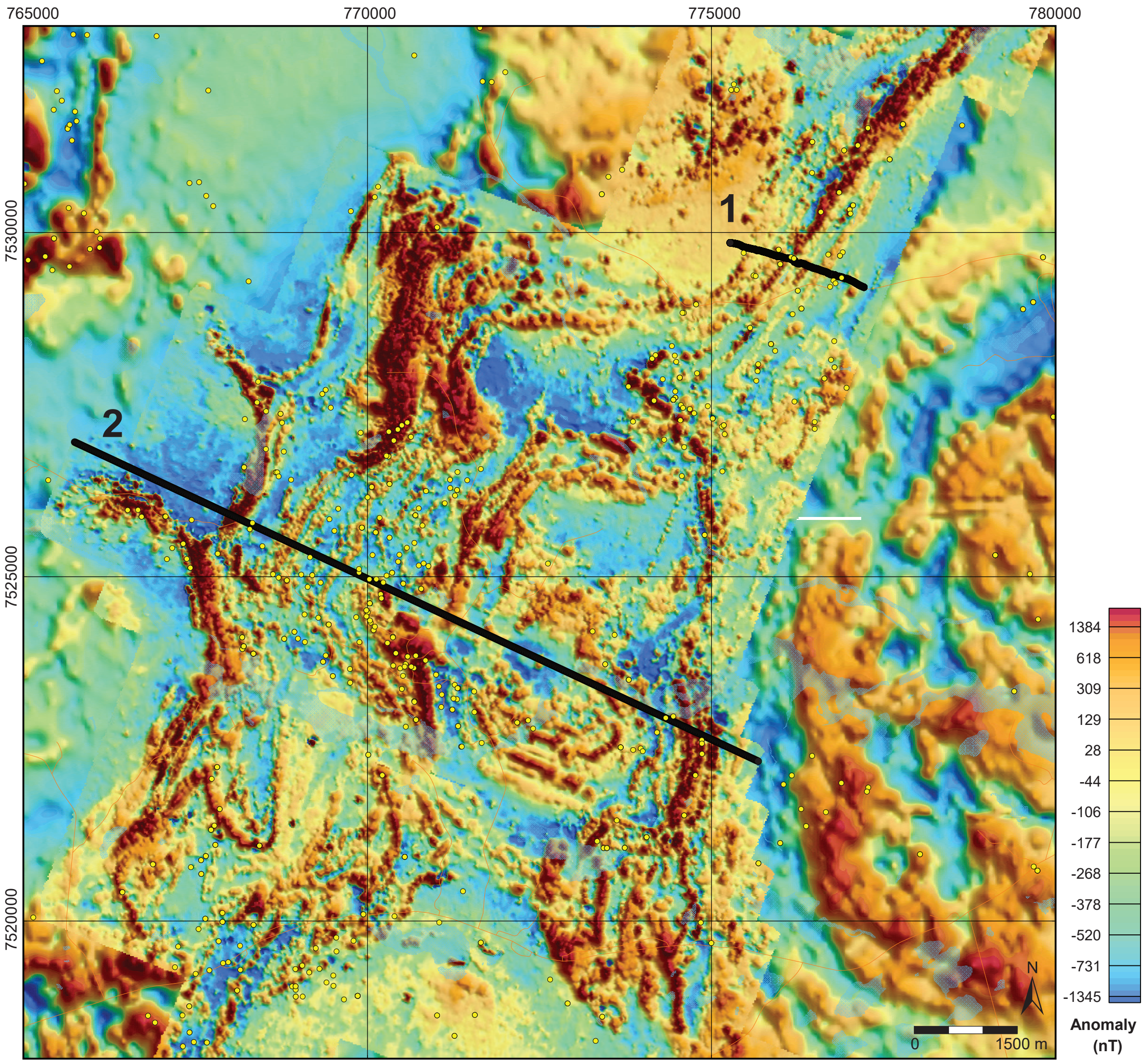

Figure 3. Magnetic anomaly map of the Nunasvaara area. Airborne data are overlain by ground-measured data. Yellow circles show the location of analysed petrophysical samples. Black lines show the extent of the 2D geological profiles that were interpreted from geophysical data.

in the magnetic map. The ground magnetic data also show the various folding events that the area has been subjected to. The high densities of the metavolcanic rocks and metadolerites (on average 2 958 kg/m^3 and 2 979 kg/m^3, respectively) give rise to a predominant gravity high in the area (Fig. 4). However, to generate such a pronounced gravity high, the dense rock must have a substantial depth. This is discussed further in the section on modelling aspects.

In the centre of the area, a few semicircular structures appear as local low anomalies on the gravity map. These gravity lows correlate with low-magnetic signatures and are shown on the bedrock map as

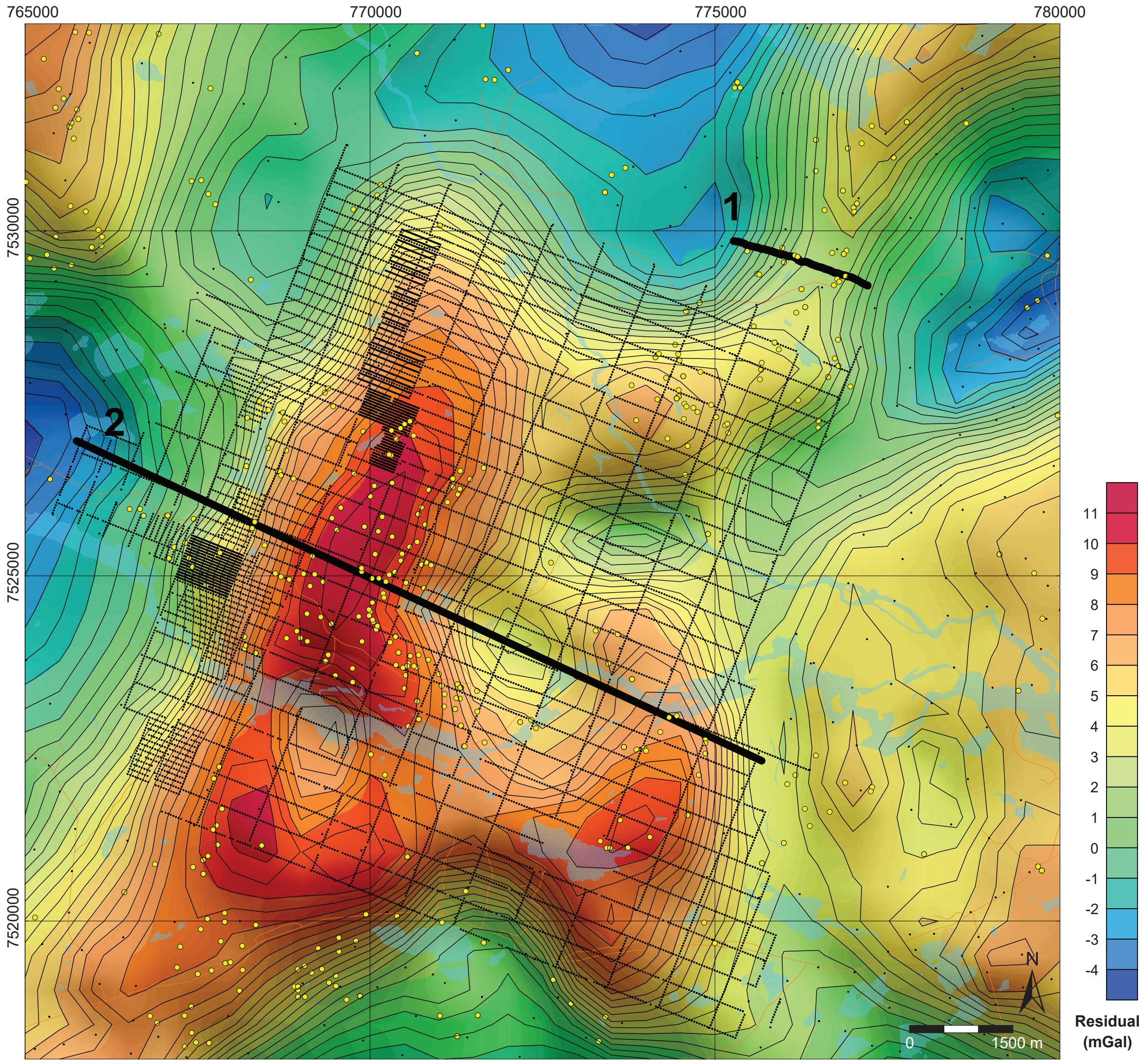

Figure 4. Residual gravity anomaly map of the Nunasvaara area. The grid of black dots represents measurement sites. Yellow circles show the location of analysed petrophysical samples. Black lines show the extent of the 2D geological profiles that were interpreted from geophysical data.

basic volcanic rocks. This appears to be an assumption, since there are no outcrops within these gravity lows, leading to considerable uncertainty about the geographical extent of this lithology. Assuming the presence of basic volcanic rocks in these gravity lows implies a shallower depth extent, underlain by less dense rocks for this lithology. Tuffs and metadolerites are present on all adjacent sides of the low-magnetic basic volcanic rock. The graphite schist horizons and their fold patterns around the central dome structure in the area are seen as narrow, conductive zones in the ground slingram data (Fig. 5).

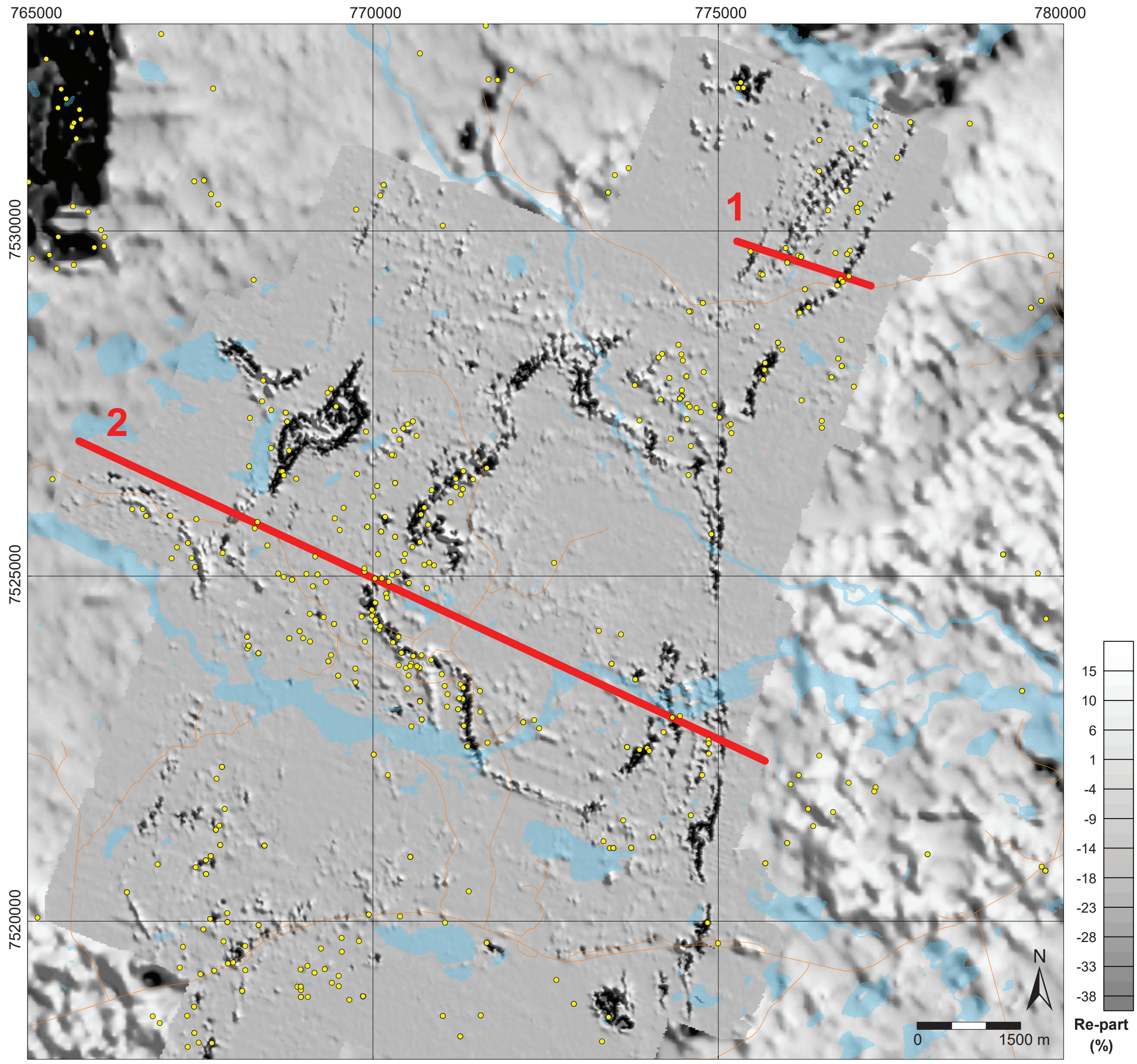

Figure 5. Slingram map of the Nunasvaara area, showing the in-phase component (Re-part). Airborne data are overlain by ground-measured data. Yellow circles show the location of analysed petrophysical samples. Red lines show the extent of the 2D geological profiles that were interpreted from geophysical data. Ground-measured VLF data were also acquired along profile "1"; results shown in Figure 7.

2D MODELLING OF PROFILE 1 AND 2

Modelling was carried out using Potent software. Background density and susceptibility have been set at 2 700 kg/m^3 and 100 × 10^{-5} SI, respectively.

Profile 1

Profile line "1" in Figure 1 and Figures 3–5 has been forward modelled based on information from newly acquired ground magnetic and pre-existing gravity measurements, together with data from analysed petrophysical samples close to the profile. This is an area where the different lithologies of the greenstones are tightly pinched between intrusive rocks on either side. VLF data were also acquired along the same profile, the extent of which crosses several black schist horizons. The results of the model are displayed in Figure 6, clearly showing the greenstones between the intrusions on either side. To gain a better understanding of the depth extent of the intrusions, the profile was extended during the modelling stage both to the northwest and the southeast to make use of regional gravity field data.

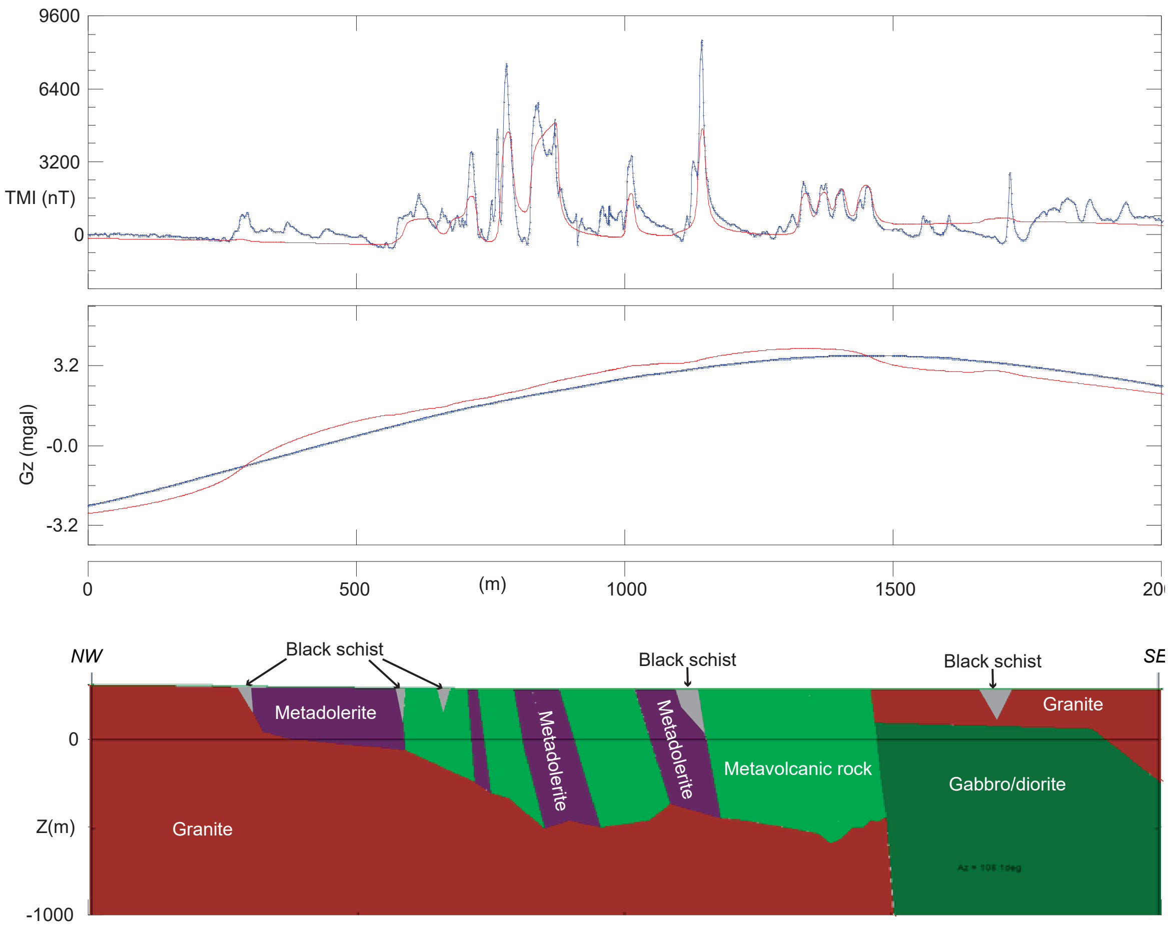

Figure 6. The modelled geological cross-section of profile "1", based on geophysical data. The cross-section is displayed from north-west (left side) to southeast (right side). The lateral extent of the profile is shown in Figure 1 and Figures 3–5. Upper: variations in the magnetic field. Middle: the gravity field. Blue lines in these boxes are observed data; red lines are the response from the model.

Model description and discussion

The gravity anomaly map (Fig. 4) shows that the profile is located across a gravity high, which strikes in a southwest–northeast direction and coincides relatively well with the basic volcanic rocks and metadolerites. The northwestern and southeastern part of the profile lie within granite intrusions from which petrophysical samples have been acquired close to the profile (red body in Fig. 6). These samples have an average density of 2 620 kg/m^3 (n = 2). Petrophysical samples acquired from the metadolerites (purple bodies in Fig. 6) and metavolcanic rocks (light green bodies in Fig. 6) in the vicinity of the profile have densities ranging from 2 800–3 200 kg/m^3 (n = 48), with an average density of 2 970 kg/m^3. This is quite uniform over the area as a whole (Table 1), with the metadolerites and the metavolcanic rocks having almost the same average densities. The assumption has been that the granite intrusion in the west continues under the greenstones, which deepen towards the east down to 800 m below ground level in the centre and east of the sequence. However, the maximum gravity anomaly along the profile is reached in the east, close to the contact with the granite intrusion. To compensate for this, a body with mafic properties has been added to the model (dark green body in Fig. 6), underlying the granite. A gabbroic to dioritic intrusive rock occurs east of the granite (Fig. 1), from which petrophysical samples have been acquired, approximately 2.5 km from the eastern end of the profile. These samples have an average density of 2 910 kg/m^3 (n = 3), which has been assigned to the mafic body. To satisfy the observed gravity data, the depth extent of the mafic body is approximately 3 km.

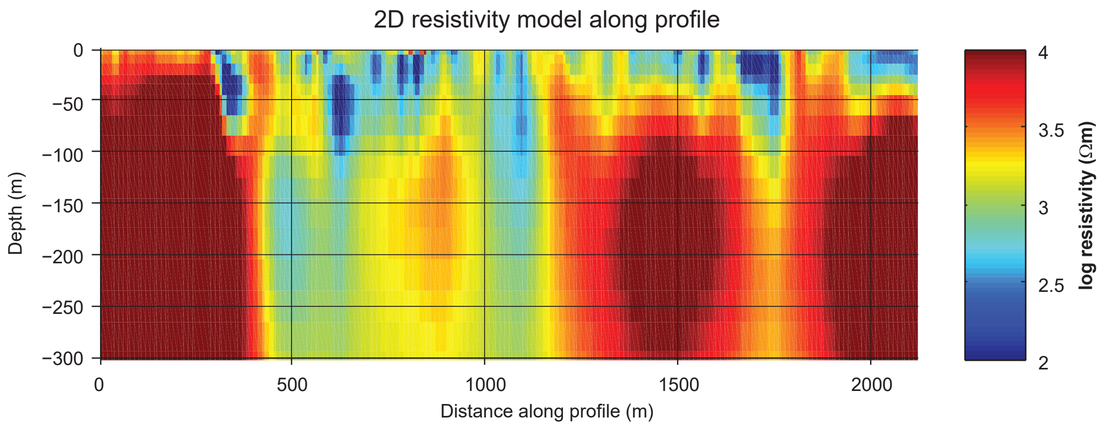

Figure 7. Resistivity cross-section along profile "1" (Fig. 1 and Figs. 3–5). The cross-section displays the resistivity properties of the shallow subsurface and is derived by inversion of VLF data.

The magnetic susceptibilities of metadolerites and metavolcanic rocks vary within a broad range over small distances, as seen in the ground magnetic data in Figure 6. The metadolerites, for instance, have magnetic susceptibilities ranging from 60×10^{-5} SI to $20\,000 \times 10^{-5}$ SI, according to data from both petrophysical samples and in situ measurements of magnetic susceptibility on outcrops close to the profile. The modelled magnetic data show that the lithologies of the greenstones dip steeply towards the east by approximately 80 degrees. The grey bodies in Figure 6 represent black schist horizons and have been adapted from the interpretation of the VLF profile, presented below.

Slingram anomalies are caused by narrow (50–100 m) black schist horizons and are aligned in the same strike direction as the magnetic anomalies. To evaluate the geometry of the black schist horizons, ground VLF measurements have been made along the profile shown in Figure 6. The results of these measurements are presented in Figure 7 as a resistivity cross-section, where the properties of the shallow subsurface are displayed. However, the exact dip and depth extents of the horizons are difficult to determine from this cross–section, since the measurements were made at only one frequency. Other factors influencing the result are the direction to the transmitter and its signal-to-noise ratio.

Several strong conductive features appear close to the surface in the resistivity cross-section (Fig. 7). Starting from the west (left side), a narrow conductive feature is located 350 m from the western end of the profile. The dip of this feature is steep towards the east and has a depth extent of approximately 100 m. This is probably the westernmost horizon of the black schist, situated at the contact between the granite intrusion and the greenstones. Continuing further east, additional conductive, vertical horizons are visible at distances of 650 m, 1 100 m and 1 750 m along the profile.

A relatively conductive segment occurs between 400–1 200 m down to 300 m below ground level. According to the slingram map (Fig. 5), this part of the profile is an area with several closely-spaced conductive horizons. It is possible that this area of multiple conductive black schist horizons causes the single broad low resistivity zone seen in the resistivity cross-section.

Profile 2

An interpreted geological 2D profile based on magnetic data (primarily ground data), gravity data and information from petrophysical samples has been created along a section crosscutting the area roughly in the middle. The geographical extent of this profile is drawn in Figure 1 and Figures 3–5 and labelled "2". The profile covers the area from the intrusion in the west, through the volcanoclastic metasedimentary rocks, basic metavolcanic rocks and metadolerites of the greenstone group to the eastern side, where it ends in intrusive rock. The resulting model is shown in Figure 8.

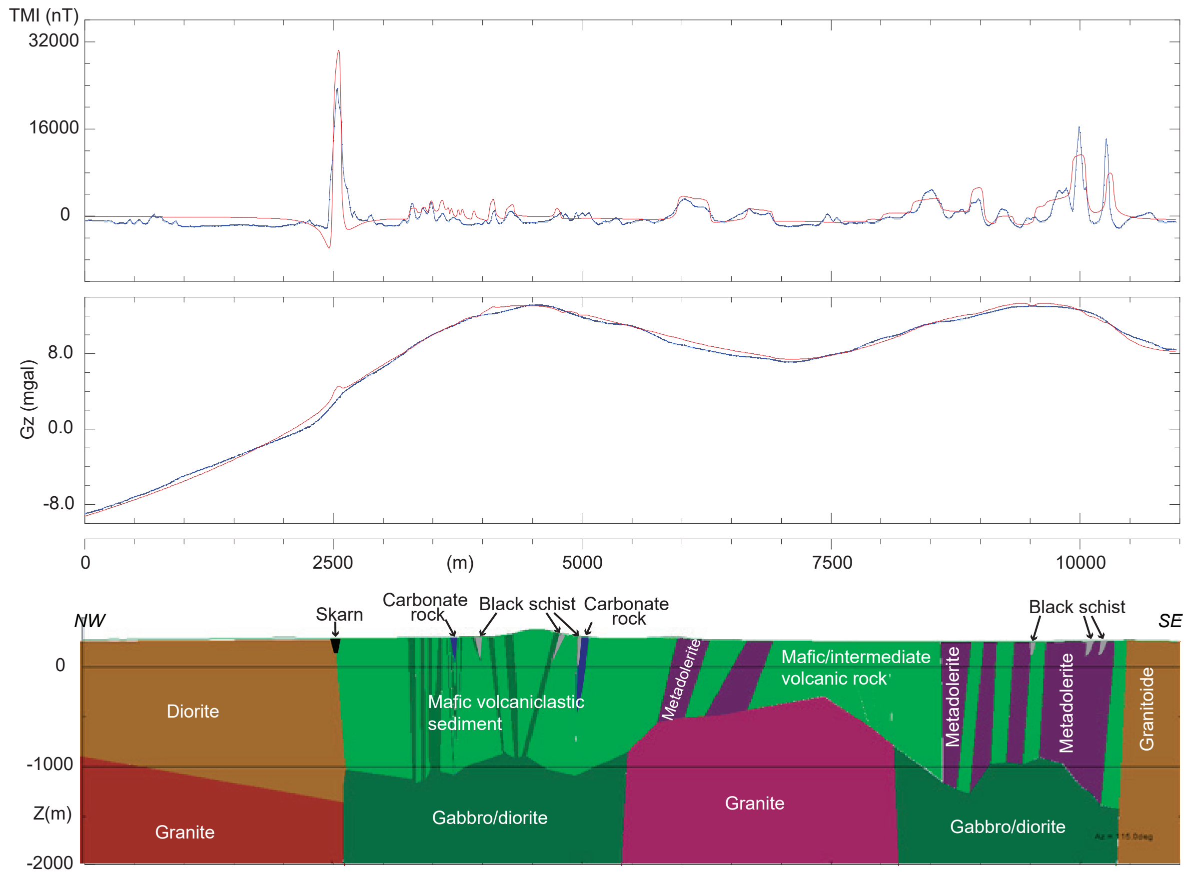

Figure 8. Forward-modelled geological cross-section of profile "2". The cross-section is displayed from northwest (left side) to southeast (right side). Upper: variations in the magnetic field. Middle: gravity field. Blue lines in these boxes are observed data; red lines are the response from the model.

Model description and discussion

The western part of the cross-section (Fig. 8) lies in an intrusion of dioritic composition, visualised as the shallower brown body. Petrophysical samples acquired from the diorite have an average density of 2 800 kg/m^3. The red body beneath the diorite is Lina granite, which has been sampled west of the profile. The samples have low densities, averaging 2 610 kg/m^3. The granite has a significant depth extent, indicated by the pronounced gravity low in the western part of the profile.

A skarn iron formation occurring at the contact between the diorite and the greenstones is clearly seen in the magnetic anomaly data. Petrophysical samples from this skarn horizon have an average density of 3 600 kg/m^3 and, for this particular location, susceptibility has been assumed to be 50 000 $\times 10^{-5}$ SI in order to fit the response from the observed magnetic field. Two samples were collected from this high-magnetic structure and have susceptibilities of 40 000 and 70 000 $\times 10^{-5}$ SI, so the assigned susceptibility is realistic. To fit the modelled response from the skarn horizon to the observed field, the structure must dip steeply to the east.

East of the skarn is a package of alternating volcaniclastic sediments of predominantly mafic composition. These lithologies are tightly stacked and folded with rapid variations in magnetic mineral content. The bulk densities of these layers are roughly similar, however, with an average density of 2 950 kg/m^3 (n = 61). This whole package is seen in the ground magnetic data as an area with short spatial distance in the east–west direction between each magnetised horizon. In Figure 8 the low-magnetic parts of the volcaniclastics are shown in light green, and the higher magnetised horizons in darker green. The high-magnetic horizons have been assigned susceptibilities in the range of

$10\,000–17\,000 \times 10^{-5}$ SI. The geometry of the magnetic layers is steep, and several have a synclinal shape. A carbonate rock occurs within the sequence (blue in Fig. 8), at approximately 3 750 m along the profile. A possible interpretation from the model could be that the magnetic layers surrounding the carbonate form a syncline around it. A pronounced gravity high can be seen in this area (Fig. 4) and, for the model to satisfy it, there must be dense rocks continuing down to substantial depth. The assumption has been that the supracrustal rocks have a depth extent of approximately 1 km, which corresponds relatively well with the shorter-waved anomalies seen in the ground magnetic data. At greater depth, a mafic intrusive (dark green in Fig. 8) has been adopted in the model, which, to satisfy the gravity high, continues down several km. The average density of the petrophysical samples analysed from the gabbro/diorite is 2 954 kg/m^3 (n = 54; Table 1), so this value has been assigned to this deep-seated lithology.

Highly magnetised metadolerites (purple colour in Fig. 8) occur between 6 000–7 000 m along the profile, which can be clearly seen on the magnetic anomaly map (Fig. 3). In situ measurements on outcrops show the average magnetic susceptibility of the metadolerites to be $28\,000 \times 10^{-5}$ SI (n = 24).

East of the metadolerites is an area of low-magnetic mafic to intermediate volcanic rock (light green in Fig. 8). This area has low exposure of outcrops. These lithologies are therefore assigned the average density value of all analysed petrophysical samples acquired from volcanic rocks in the model: 2 960 kg/m^3 (Table 1). On the gravity map (Fig. 4), this part of the profile corresponds to an area with a local, semicircular low-gravity anomaly. To achieve a model that is relatively consistent with the observed gravity field, there must be a less dense lithology underlying both the highly magnetic metadolerites and the dense volcanic rocks between 5 500–8 000 m along the profile. The assumption during the modelling process has been that the underlying rock is a granitic intrusion (pink in Fig. 8), with the same physical properties as the one closest to the southern border of the greenstone package (Fig. 1). The deep-seated granitic intrusion has thus been assigned a density of 2 650 kg/m^3 and a susceptibility of 100×10^{-5} SI. In the model, the shallower metadolerites and volcanic rocks extend approximately 600–1 100 m below the surface, while the intrusion continues down to a depth of several km to satisfy the observed gravity field.

East of the low-magnetic volcanic rock is another area with banded magnetic structures making up a semicircular pattern around the low-magnetic volcanic rocks. These high-magnetic bands are mainly caused by metadolerites (purple in Fig. 8), with magnetic susceptibilities up to $40\,000 \times 10^{-5}$ SI, and appear to have a steep dip closest to the low-magnetic volcanic rock, with a tendency to dip more to the west closest to the eastern rim of the greenstone package. There are also strongly conductive horizons in the area, clearly seen in the slingram data (Fig. 5), caused by black schist horizons. A high-gravity anomaly is associated with this area (Fig. 4); the amplitude indicates a substantial depth extent of the dense rocks. Available petrophysical information shows the densities of the shallower greenstones are within the range 2 900–3 000 kg/m^3 in the area. By applying magnetic and density properties derived from samples to the shallow bodies in the model that represent the greenstones, a good fit is achieved to the shorter-waved ground magnetic data, suggesting a depth extent of the metadolerites and metavolcanic rocks of approximately 1 km below ground level. Ending the greenstones at this depth, however, creates a mass deficiency in the gravity response compared with the observed data. A mafic intrusive (dark green in Fig. 8) has therefore been adopted in the model below the greenstones to compensate for this. Using a density of 2 954 kg/m^3 for this body, which is the average density for gabbro/diorite in the area (Table 1), the mafic intrusive has a depth extent of several km below ground level.

The bedrock east of the greenstones consists of intrusions. Closest to the greenstones is an intrusion with relatively low average density, 2 750 kg/m^3 (brown in Fig. 8).

MASUGNSBYN

Geological introduction

The bedrock in the Masugnsbyn area consists of basaltic metatuff belonging to the *Veikkavaara greenstone group*, overlain by metavolcanic and metasedimentary units (chert, mafic schist and marbles) belonging to the *Kalixälv* and *Pahakurkio groups* (Padget, 1970). Metadolerite and graphitic black schist occur in the metatuffs. Intrusive rocks of mainly granitic to syenitic composition have intruded the supracrustal rocks, and gabbroic rock is also present (Fig. 9). Skarn iron, dolomite, Cu-Zn-Pb, Cu-Au, and graphite mineralisations occur in the area. A more detailed description of the geology and lithostratigraphy around Masugnsbyn is found in Lynch et al. (2018).

Geophysical interpretations in the Masugnsbyn area

Geophysical data coverage is extensive around Masugnsbyn. Airborne magnetic, radiometric, VLF and slingram data all exist, as well as regional ground gravity data. The area is well covered by various ground geophysical measurements targeting, mainly, exploration objects in previous campaigns. For more information on airborne and ground geophysical data the reader is referred to the report by Hellström & Jönsson (2014).

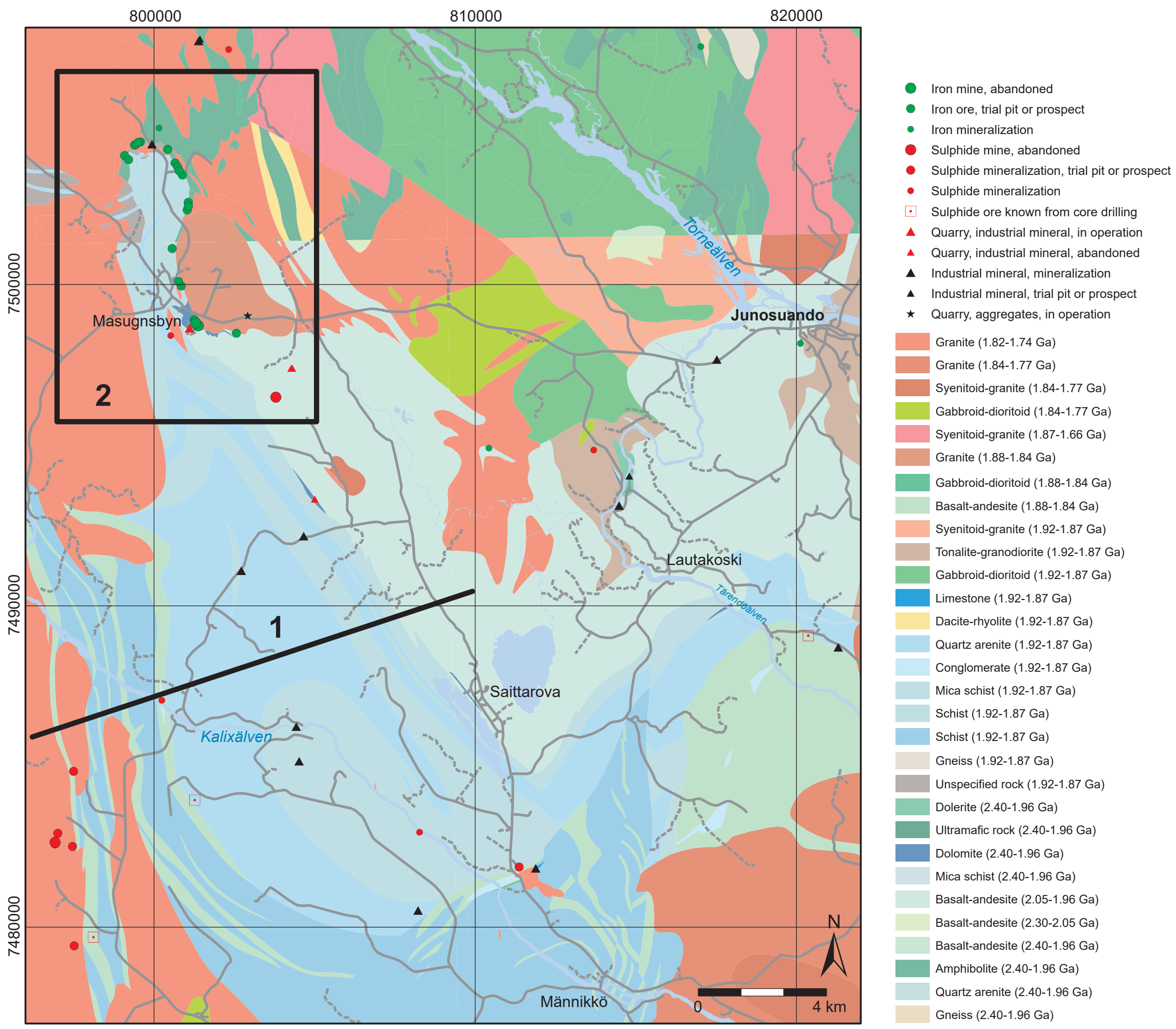

Figure 9. Bedrock map of the area around Masugnsbyn, after Bergman et al. (2012). The mineralisation occurrences are shown on the map. The areas targeted for modelling lie along the profile "1" and within the polygon "2".

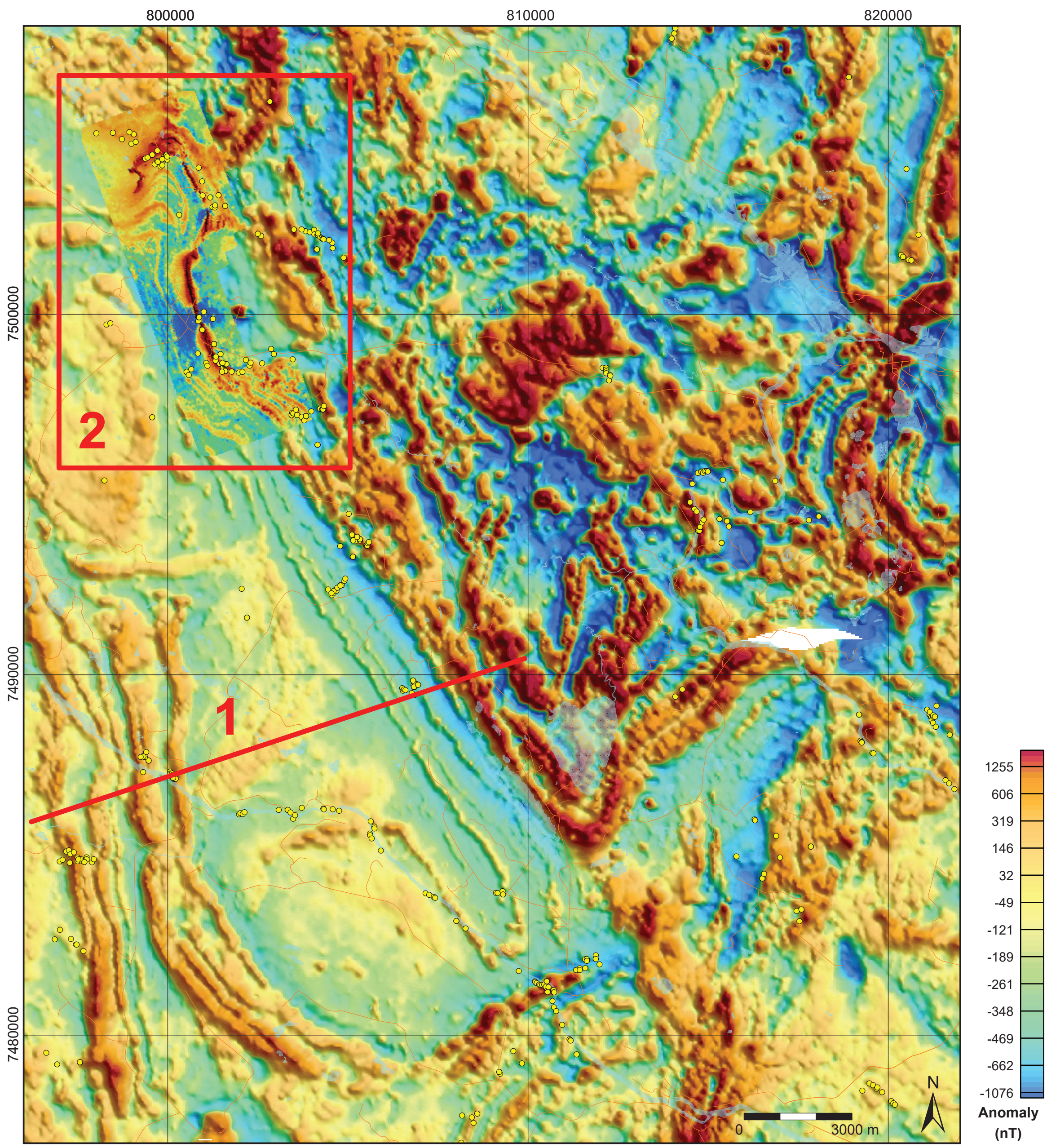

Figure 10. Magnetic anomaly map of the Masugnsbyn area. Data from ground magnetic surveys around the Masugnsbyn ore deposit are transposed onto the airborne data. Yellow circles show the location of analysed petrophysical samples. The areas targeted for modelling lie along the profile "1" and within the polygon "2".

The overall pattern of magnetic (Fig. 10) and gravity field data (Fig. 11) represents the lithological units in the area. In the most westerly part, the bedrock predominantly consists of metasedimentary rocks of the *Kalixälv* group, with intercalations of basaltic to andesitic metavolcanic rocks. The metavolcanic rocks have a higher magnetic susceptibility and can be outlined with the aid of the magnetic field pattern. The metasedimentary *Pahakurkio* group predominates in the central parts of the area. These rocks are characterised by low magnetic susceptibility and low to intermediate density. Several long, narrow and weakly positive magnetic anomalies within this sedimentary unit may represent original layering. The eastern part of the area has a high-magnetic signature and an obvious V-shaped

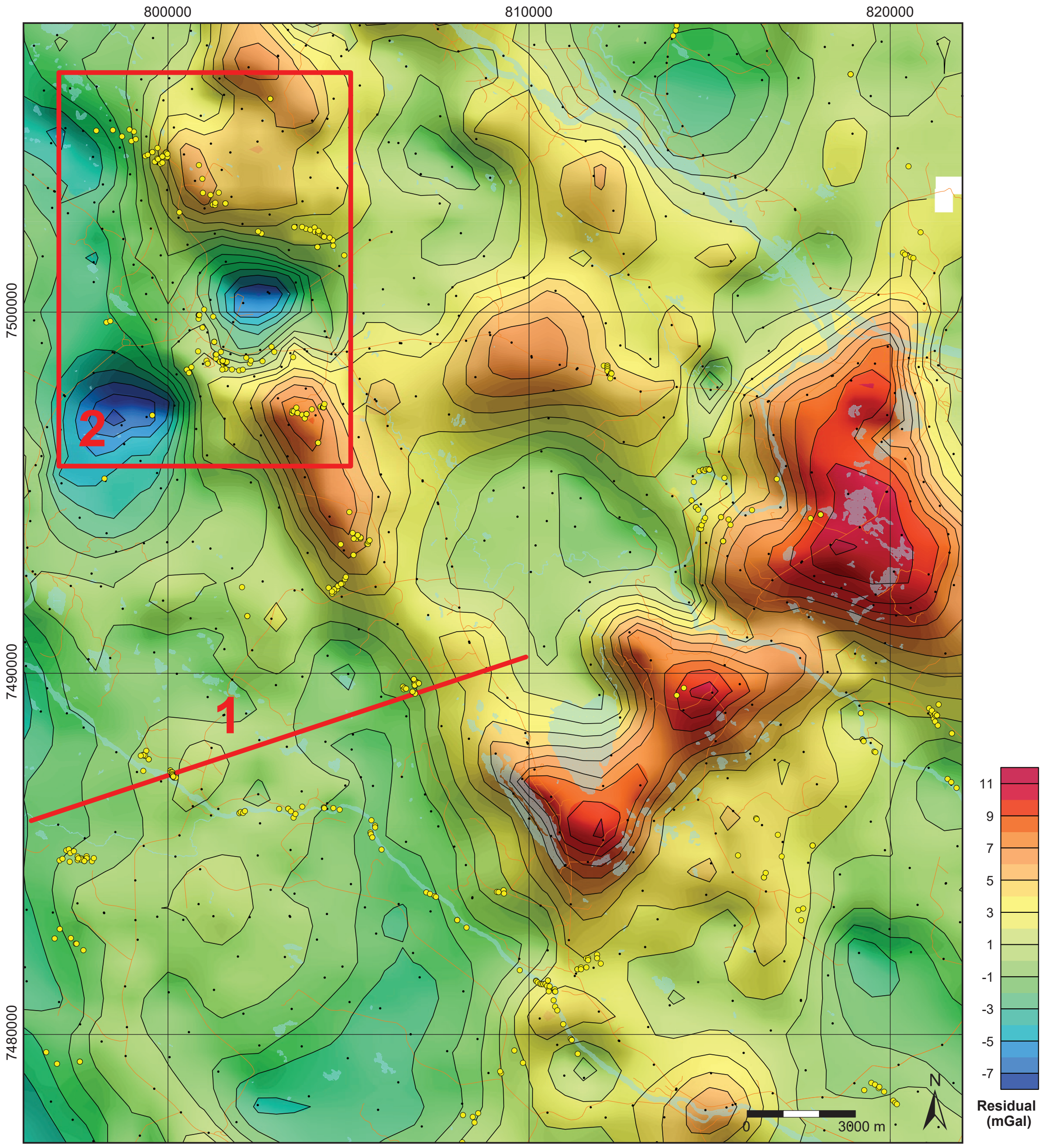

Figure 11. Residual gravity map of the Masugnsbyn area. Yellow circles show the location of analysed petrophysical samples. Black dots represent regional measurement sites. The areas targeted for modelling lie along the profile "1" and within the polygon "2".

fold, which can also be observed in the gravity and slingram data. The observed patterns are due to the Veikkavaara greenstone group consisting of basaltic greenstone with graphitic schist and carbonate horizons. The graphitic schist horizon is evident in the electromagnetic geophysical data (VLF and slingram), which outline the conducting horizon well (Fig. 12). The geophysical and petrophysical data is further presented and described in Hellström & Jönsson (2015).

Geophysical modelling in the Masugnsbyn area has been carried out in two areas; see Figures 9–12. The first area of interest is the Masugnsbyn iron ore, where dense sampled gravity data, together with information from petrophysical samples and boreholes, have been used as input data to construct 3D models of the anomalies hosting the mineralisation. Ground magnetic and slingram data have been used to quantify the dip of these lithologies at depth. The second area of interest is the regional geological setting across the sedimentary basin, which is surrounded by granite in the southwest and mafic volcanic rocks in the northeast. In this regional model, airborne magnetic data were primarily used as input data, along with information from petrophysical samples. At some locations, newly acquired geophysical data were also used during the modelling stage to resolve more details in the subsurface conditions.

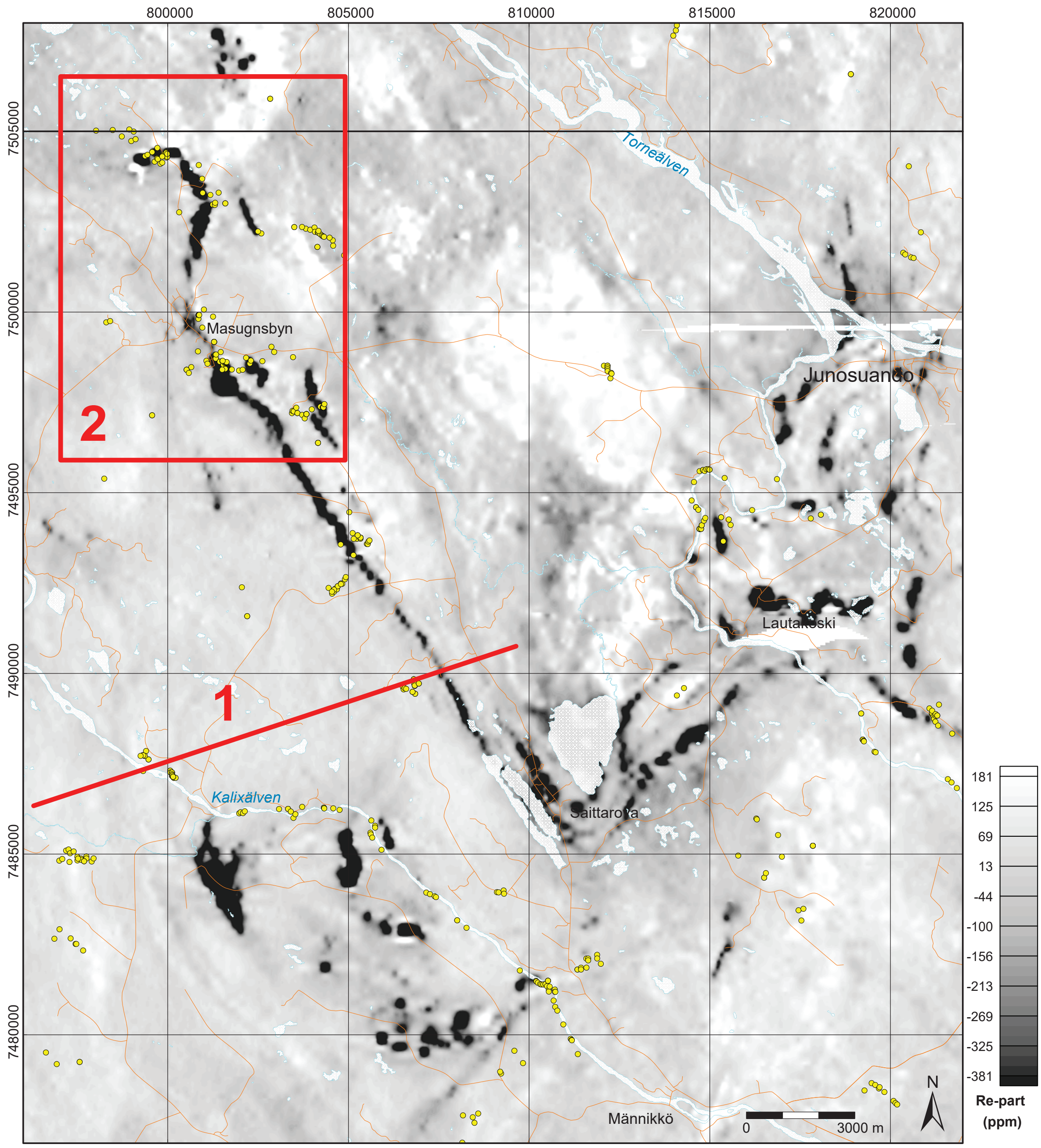

Figure 12. Slingram map of the Masugnsbyn area showing the in-phase component, based on airborne measurements. Yellow circles show the location of analysed petrophysical samples. The areas targeted for modelling lie along the profile "1" and within the polygon "2".

3D modelling of the Masugnsbyn iron ore

Geophysical modelling of the Masugnsbyn iron ore deposit was carried out with the aim of visualising the ore body in 3D. The final model was then compared with the results from the numerous boreholes in the area to build a 3D geological model. The Masungsbyn iron ore is a well-known and well-explored area. A historical and geological description of the area and references to earlier publications are presented in Hellström & Jönsson (2014). Detailed gravity and magnetic surveys were conducted between 1963 and 1967; slingram measurements were carried out in 1974.

Model description

The model was constructed from inverse modelling of gravity field data and has been generated in the VOXI environment, an extension of the Geosoft software package. The gravity data used as input data for the model were acquired by SGU in 1964–1965 and consist of terrain-corrected Bouguer anomaly data. The line/point distances vary within the area: from 320 m/40 m to 40 m/20 m over the ore body. The densest sampled areas have been modelled separately to maximize the model resolution (called North and Central part in Fig. 13). The different modelled areas are shown in Figure 14, the southern

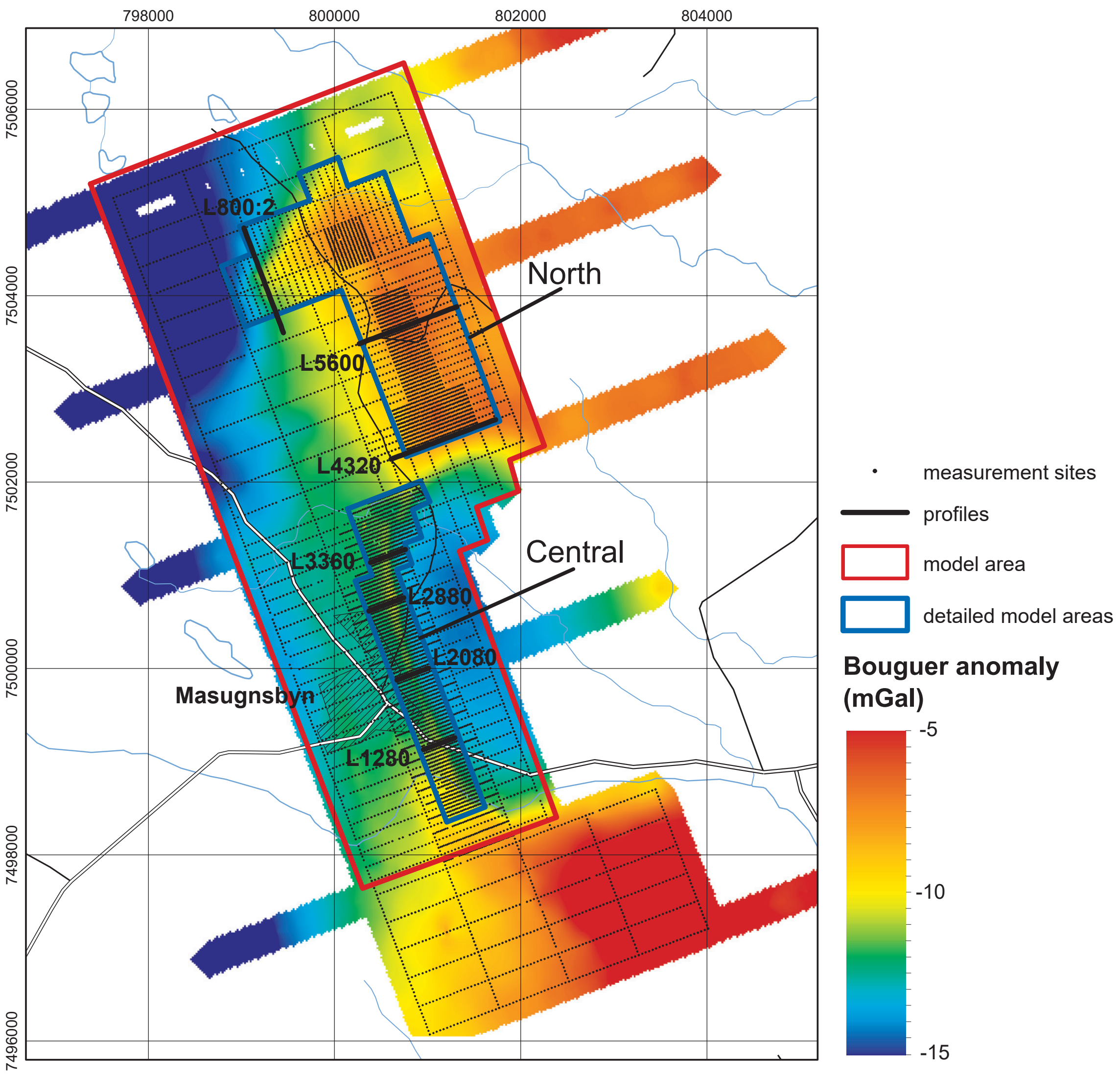

Figure 13. Dense gravity measurements in the Masugnsbyn iron ore area. The map extent corresponds to polygon “2” in Figures 9–12.

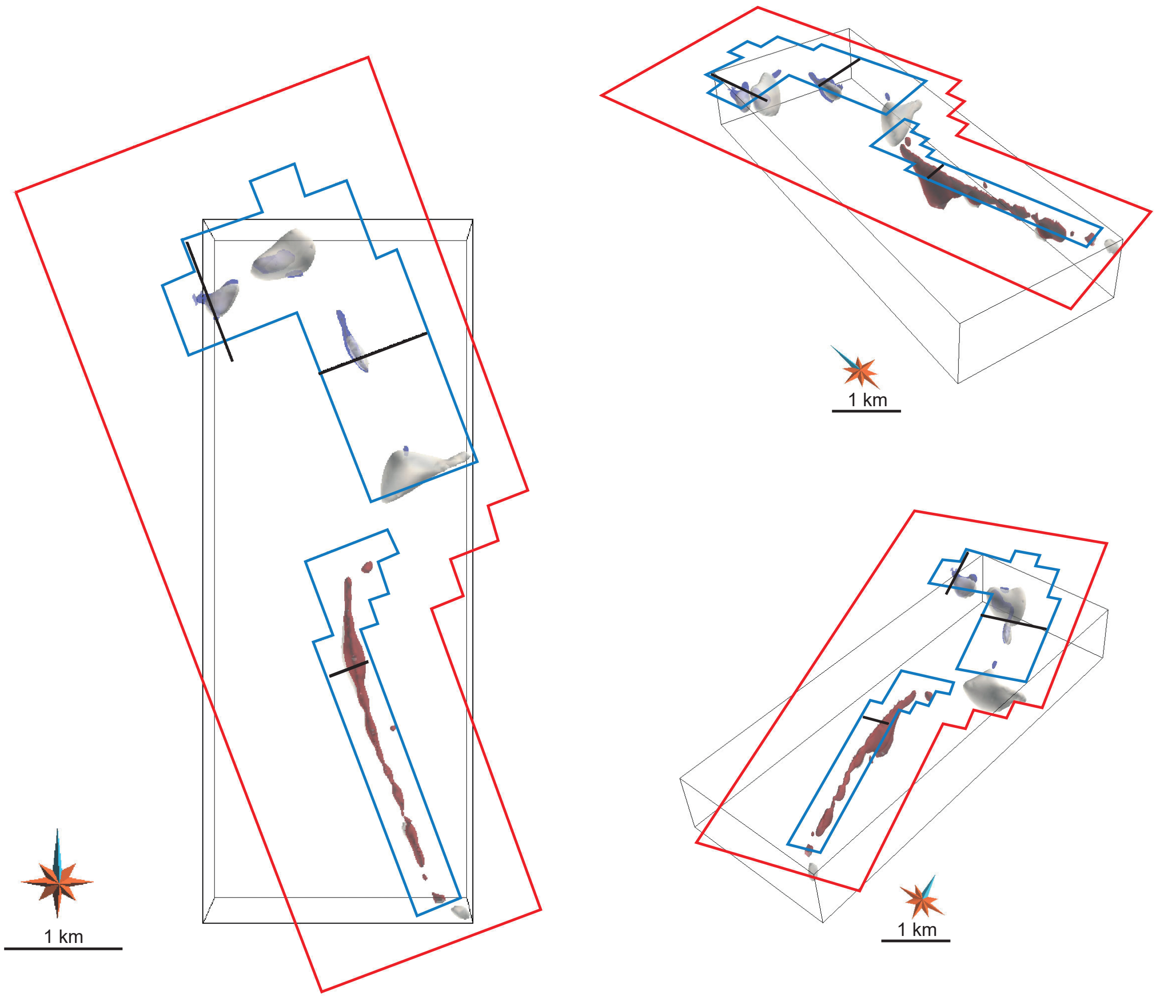

Figure 14. The modelled density distribution seen from different perspectives. The red polygon defines the area modelled, with the two subsidiary modelled areas North and Central (blue). The black lines show the location of the profiles in Figure 16. The grey isosurface represents a density value of 3 000 kg/m³, the blue 3 020 kg/m³ and the red 3 100 kg/m³. The dimensions of the black box are: x: 2 600 m, y: 6 700 m and z: 1 200 m. Visualisation in GOCAD software.

part covering the Junosuando field and the northern area including Vähävaara, Välivaara, Vuoma and Isovaara. The models are restricted to values between 2 200–3 700 kg/m^3, as the background density is attributed to 2 700 kg/m^3. Petrophysical samples acquired and analysed in 2015 show that the skarn iron ore has a density range of 3 300–4 500 kg/m^3.

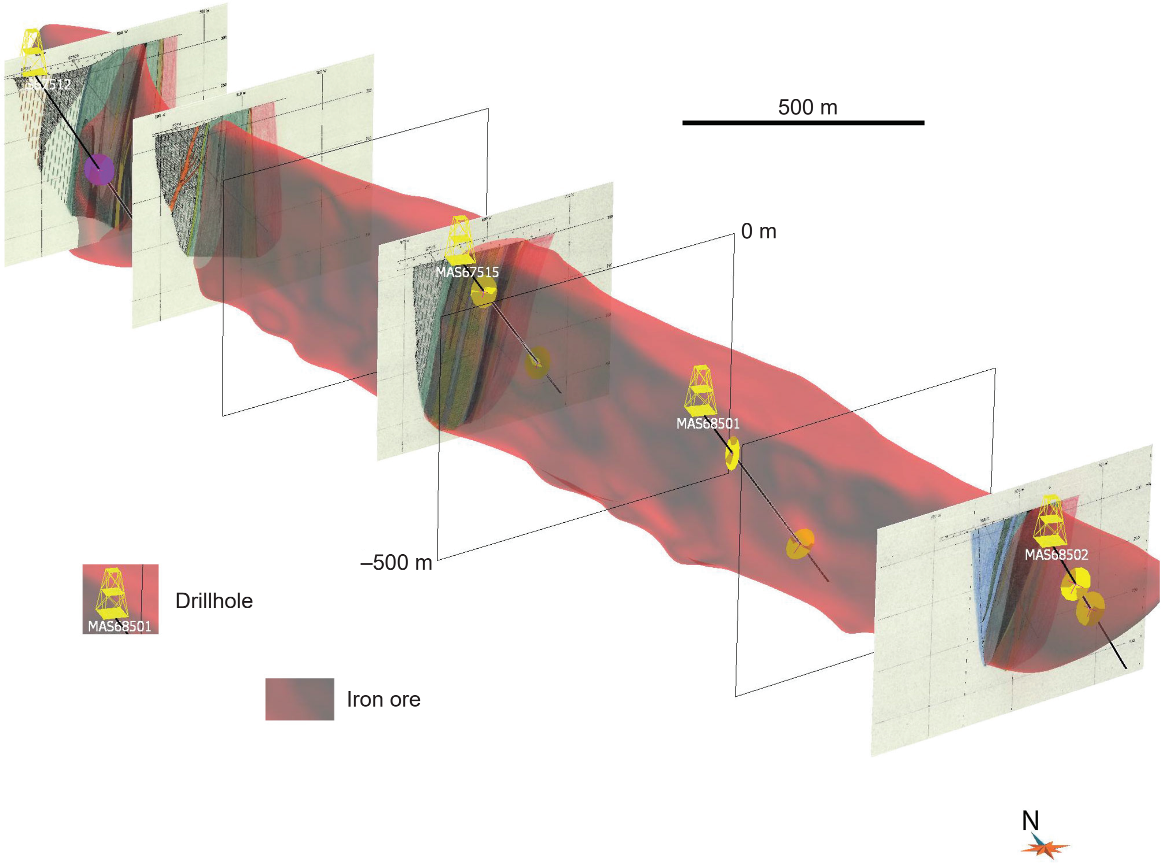

Figure 15. Established southern part of the Masugnsbyn iron ore body based on surface modelling using a series of geological profiles and drill core data. The profiles were published earlier by Witschard et al. (1972). Note the similarity between the geometries of the mineralised skarn and thin ore body obtained in this model and the geometries of the density isosurfaces displayed in Figure 14. Hollow frames refer to the locations of the non-displayed profiles, which were also used to constrain the outline of the ore body. Drill markers (yellow discs) indicate the outer contact with the ore body. Visualisation in GOCAD software.

Result

The result of the modelling is shown in Figure 14, where three isosurfaces visualise a possible density distribution that would yield the observed gravity field. The surfaces are constructed from the three model areas (Fig. 13) and have the same data but different resolutions, yielding a slightly different result. These surfaces correlate well with earlier interpretations of the subsurface density distribution. According to Witschard et al. (1972), the ore zone in the Junosuando field is between 70 and 100 m wide and dips steeply to the west (Fig. 15). The model shows a width between 50 and 150 m for the mineralised skarn, represented by a vertical slab (central model). In Figure 16 the gravity response along three profiles is shown to illustrate the result of the model, as well as the correlation between the observed gravity data and response from the modelled density distribution.

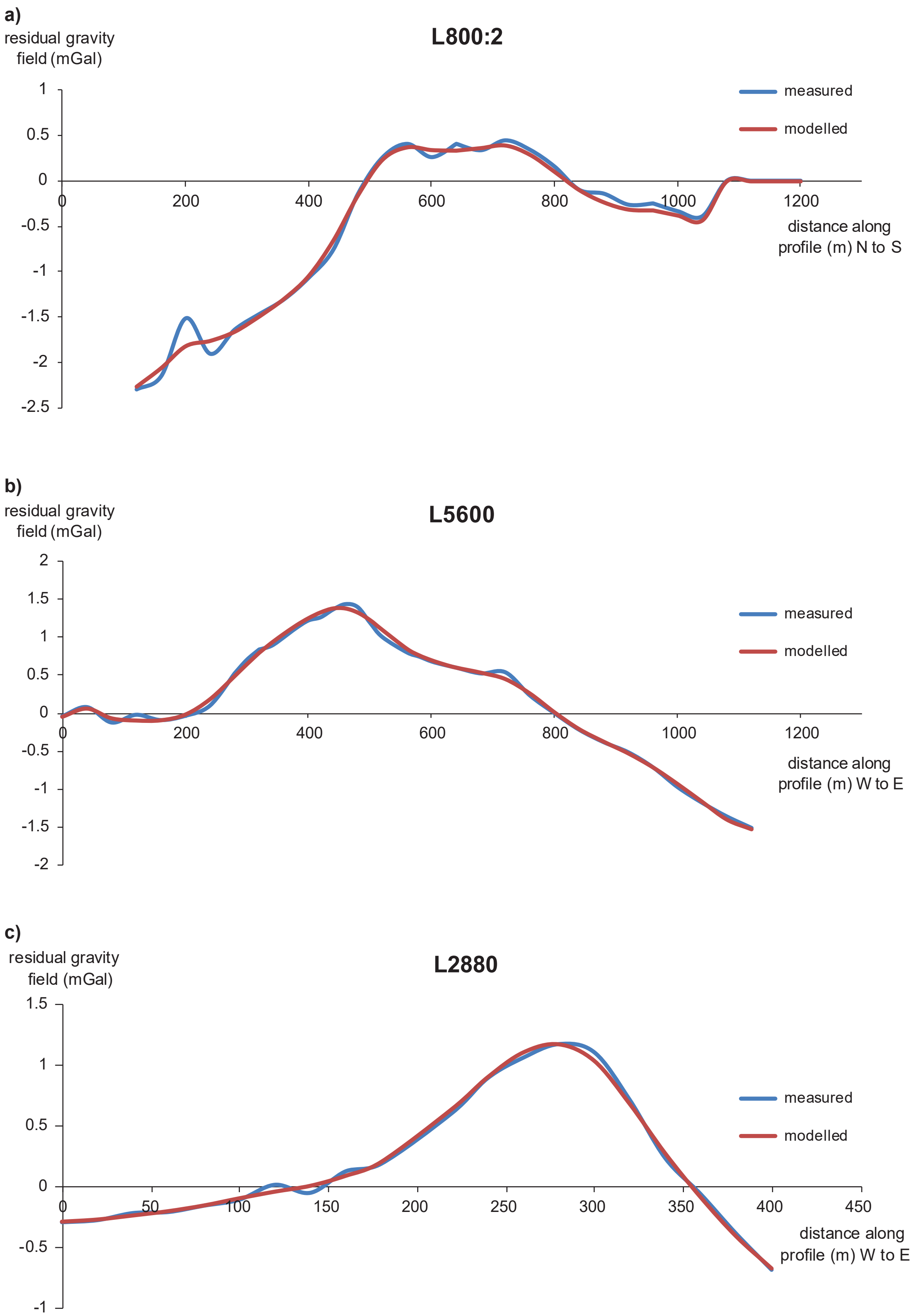

Figure 16. Comparison between measured gravity data and response from the model along three profiles. The profiles L800:2 (a), L5600 (b), and L2880 (c) correspond to those displayed in Figure 13.

REGIONAL MODELLING

Introduction

The structural domain in which the Masugnsbyn area is located shows variable foliations and complexly folded rocks. A detailed description of the geological setting can be found in Lynch et al. (2018) and Grigull et al. (2018). The bedrock map from Padget (1970) uses four cross-sections to illustrate different structural, tectonic and lithological relationships. The extent to which geophysical information was used during the modelling stages to produce these profiles is not known. Profile I (Figs. 9–12 and 17) is of two of the main tectonic features in the area; the *Kalixälv dome* and the *Masungsbyn syncline*.

A regional geological model, based on geophysical data and petrophysical information, has been constructed along Profile I and its closest surroundings. Both previously and newly acquired geophysical data have served as input data to develop a structural and lithological interpretation of the area. Airborne magnetic data are primarily used together with magnetic properties of analysed petrophysical samples or in situ measurements of magnetic susceptibility on outcrops. The model has been further refined in those areas where new ground magnetic or VLF data have been acquired.

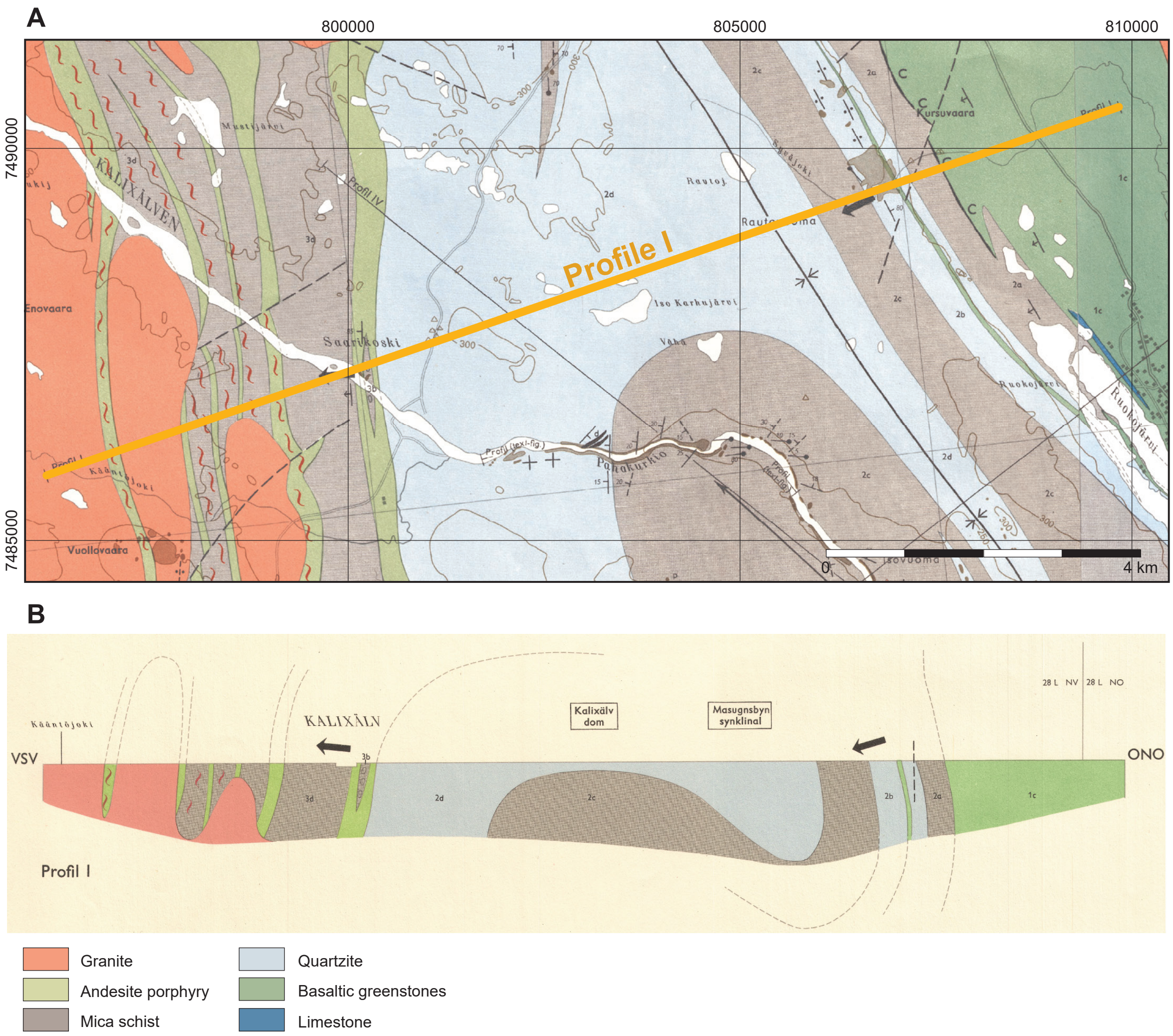

Figure 17. The location of Profile I on the bedrock map (A) and its vertical section (B), both from Padget (1970). The length of the profile is 14.6 km and the depth extent of the cross-section is approximately 1 km.

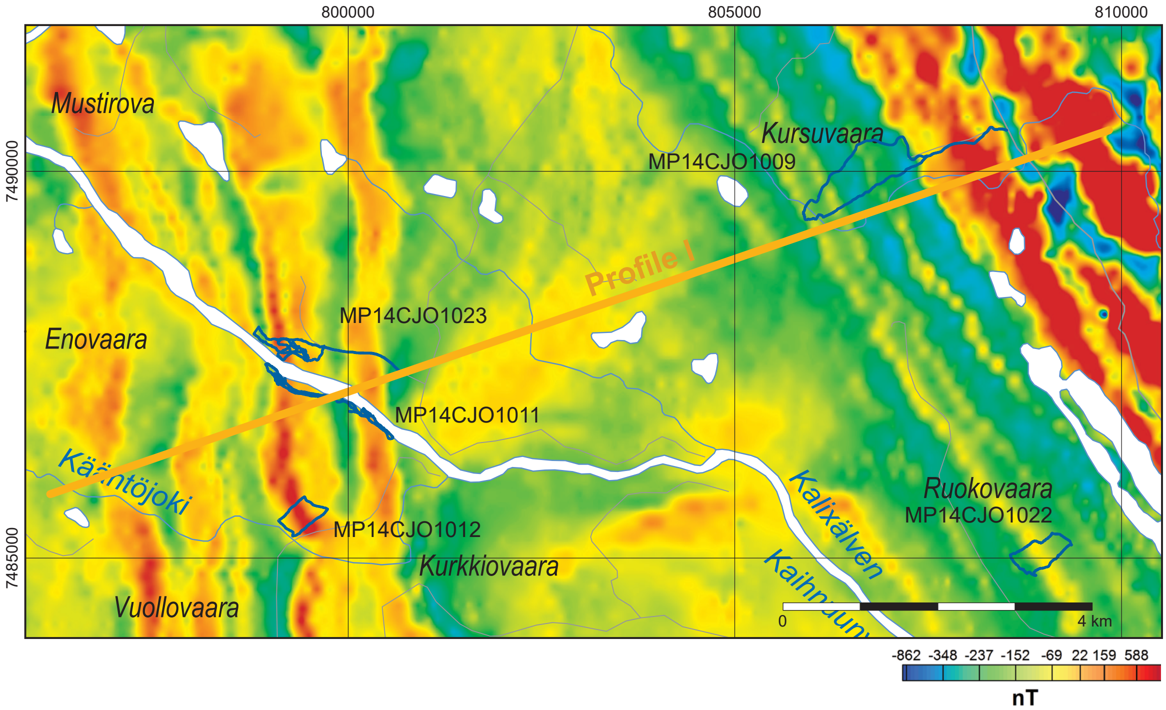

Figure 18. The magnetic anomaly field together with the location of newly acquired ground magnetic profiles (blue) and the extent of the profile (Profile I) along which the model is presented.

Model description

The modelling procedure is a forward modelling concept, where bodies have been created and assigned parameters that would yield a similar response compared to the observed magnetic data. To limit the degree of freedom when creating the model, other available data have been used to restrict parameters. The model bodies generally have simple tabular geometry, assumed to represent layers or dikes within the area. Other limiting data include structural measurements and automated strike and dip calculations of the magnetic anomaly field, which provide an indication of the dip of the bodies (Bastani & Pedersen 2001). Information on magnetic susceptibility, either from in situ measurements or from analysed petrophysical samples, is of most importance in limiting the range of possible values and, together with measurements of remnant magnetisation, if prominent, its direction.

The magnetic susceptibility of the background (i.e. where there are no bodies) is set at zero. Thus, magnetic susceptibility values for the bodies presented are relative values compared with the surrounding rocks. The depth extent for all bodies is set at approximately 1 km. Bodies have been grouped according to the anomaly in the magnetic field pattern to which they belong. This may correlate to different bedrock types or different magnetic characteristics within a bedrock type (Figs. 18 and 19a).

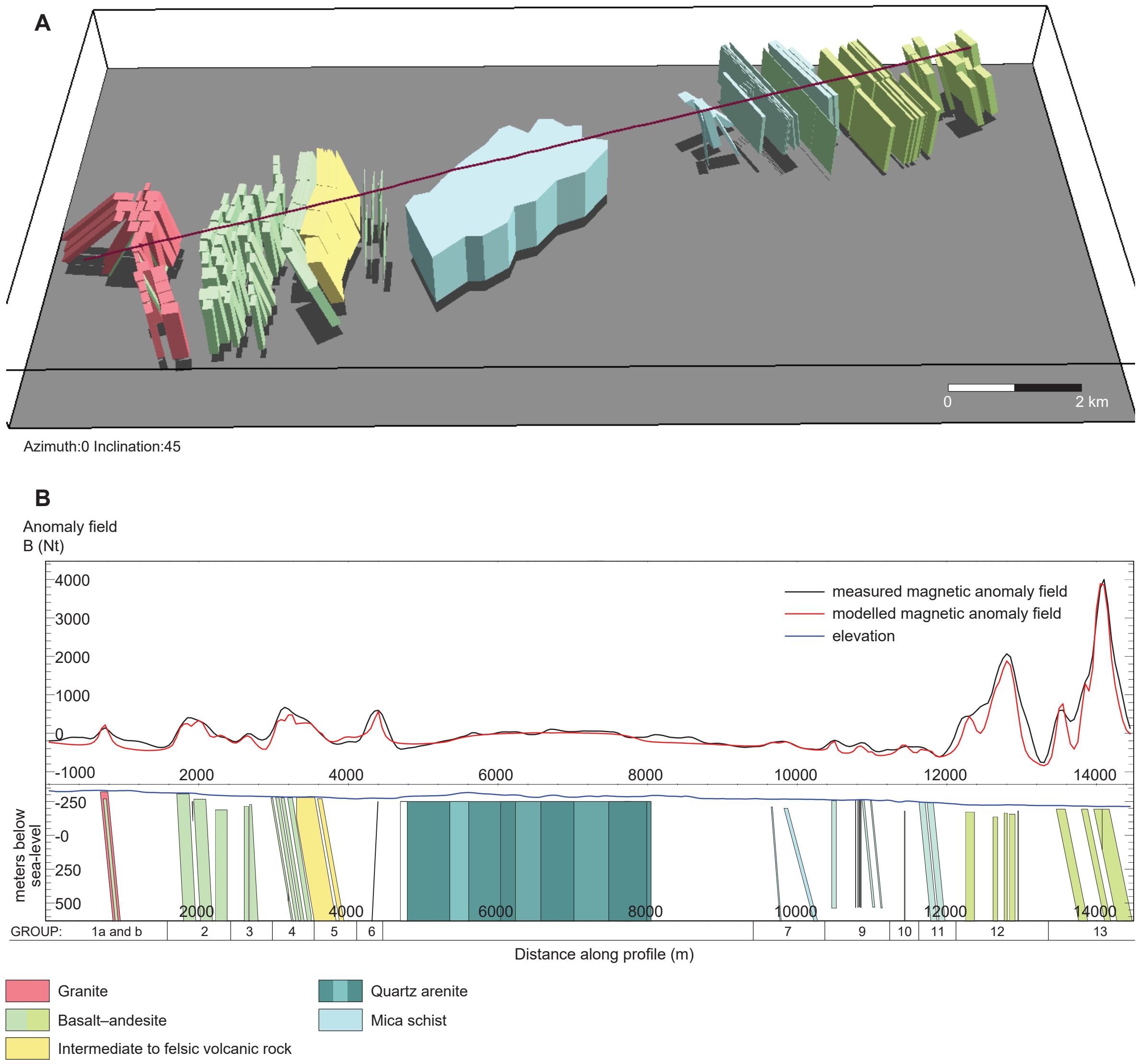

Figure 19. The results from the forward model based on geophysical data. **A.** shows the bodies in perspective with the modelled profile outlined, and **B.** shows the modelled response (red) compared with the measured magnetic anomaly field (black) and the cross-section of the bodies below. Note the different horizontal and vertical scales in B.

Results

The spatial geometry and distribution of bodies are shown in Figure 19a). The measured and the modelled response from the bodies are shown in cross-section in Figure 19b). The outline of the modelled bodies at the surface is shown in Figures 20a) and b). The bodies have been divided into different groups, depending on which anomaly and assumed lithology they represent. The magnetic susceptibility distribution for the different groups is shown in Figure 21.

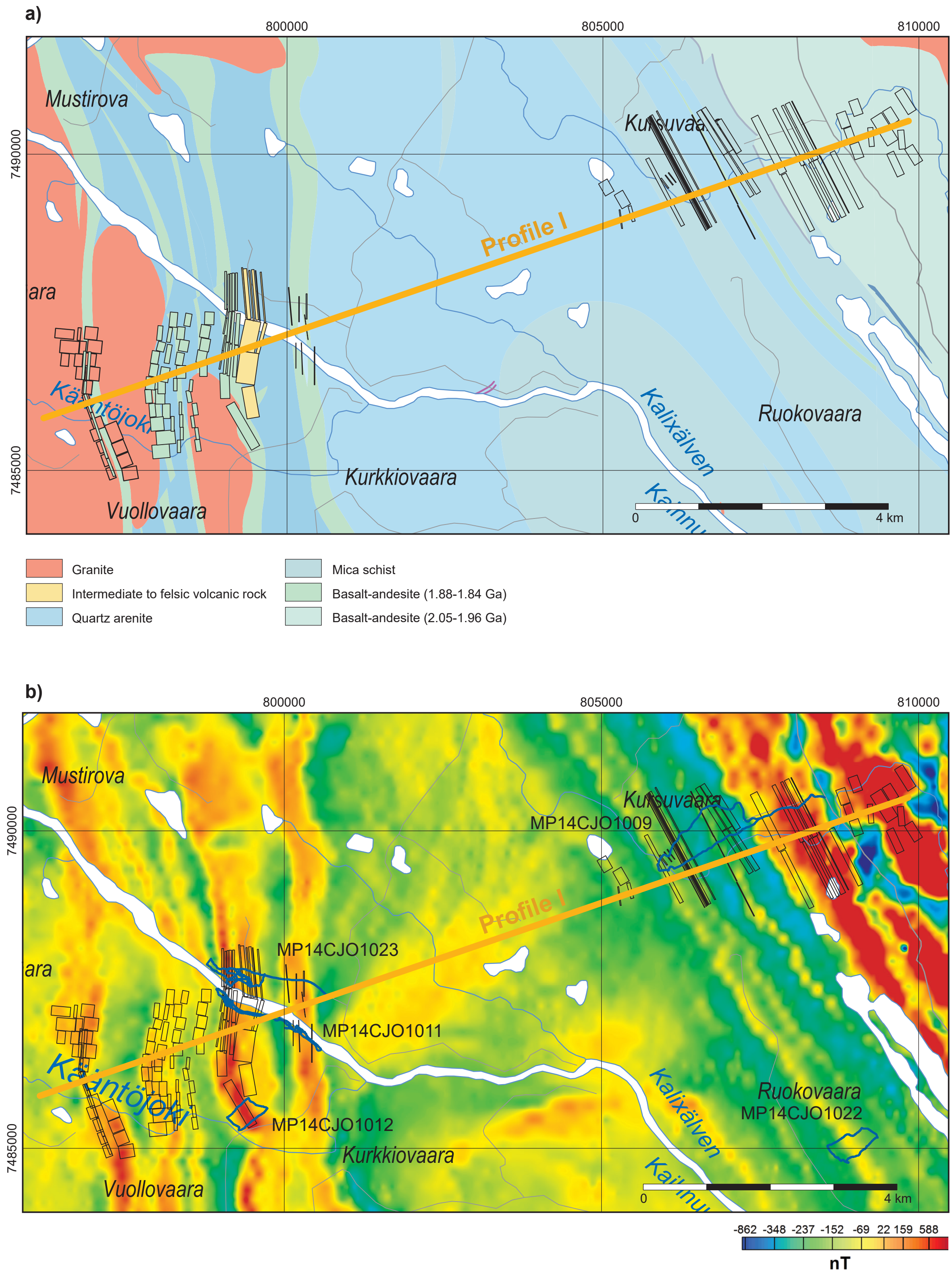

Figure 20. The location of the modelled bodies at the surface compared with the bedrock map a) and the magnetic anomaly map b). The bedrock map is from Bergman et al. (2012).

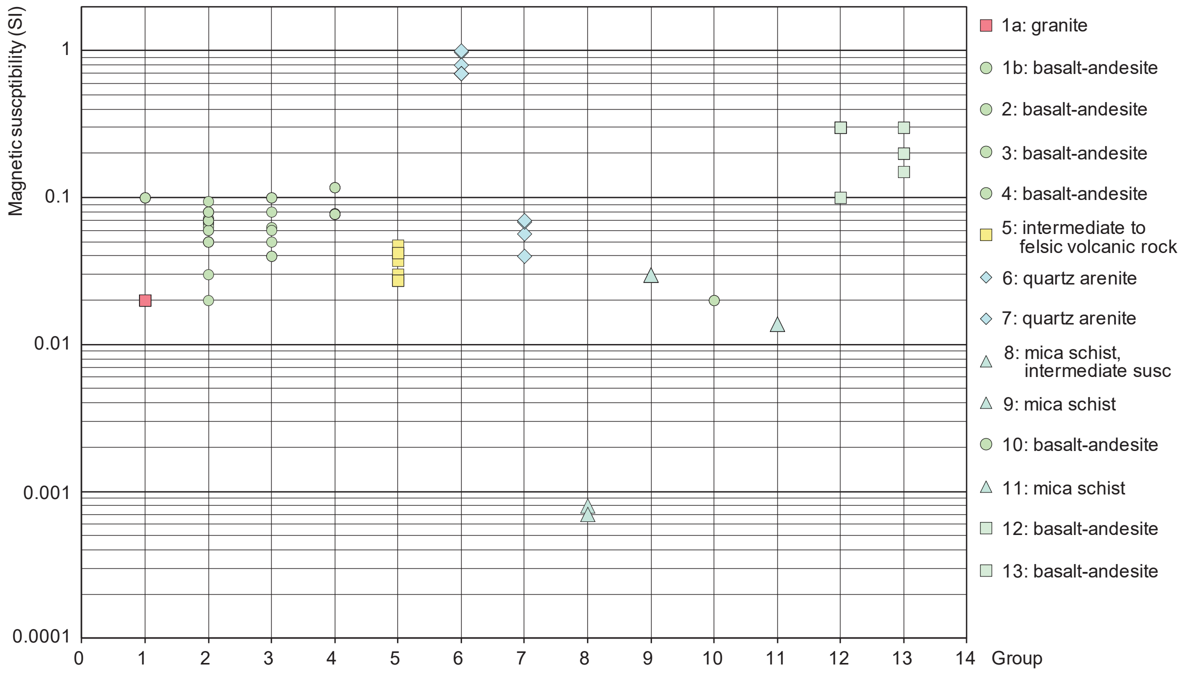

Figure 21. Magnetic susceptibility distribution within the different groups of bodies corresponding to those in Figure 19.

Description of the model and discussion

Field observations and petrophysical analysis of the granite in *Group 1* show there is a significant variation of the magnetite content, with increasing magnetic susceptibility adjacent to andesitic horizons. Three petrophysical samples from the granite gave a susceptibility range of 0.0016–0.021 SI while one sample from the copper mineralised andesite has 0.15 SI. On this basis, and compared with the observed magnetic field, the horizon must have a dip close to vertical.

There is considerable uncertainty about the physical and geometric properties of *Groups 2 and 3* due to the lack of field data or geophysical constraints. Instead, the assumption has been that the magnetic anomalies are caused by similar andesite to *Group 1*, but intercalated in low-magnetic sedimentary bedrock. A VLF profile of this area shows two distinct vertical horizons with high electrical conductivity (blue areas in the profile in Fig. 22B).

The basic volcanic rocks in *Group 4* are modelled on the basis of newly acquired ground magnetic data (Fig. 23), whose geographical extent in shown in Figure 20b). The data indicate that magnetic anomalies are caused by several thin, 20–60 m, tightly spaced slabs dipping 75 degrees to the east. The total width of this package is approximately 150 m.

Group 5 consists of volcanic rocks whose composition ranges from intermediate to felsic (Fig. 24A). The ground magnetic data indicate that magnetic horizons are 10–60 m wide, with a total width of 200–300 m for the entire unit of volcanic rocks. The geometry of these horizons is assumed to be concordant with group 4, i.e. an approximate dip of 75 degrees to the east (yellow bodies in Fig. 23).

Field observations of lithologies in *Group 6* show that this part of the profile consists of fine-layered arenite with highly variable magnetic susceptibility (Fig. 24B), which in itself may explain the enhanced magnetic anomalies in the area. Locally, susceptibility values over 1 SI have been observed in outcrops. The geometry of the highly magnetised horizons is determined by automated calculations on the magnetic anomaly pattern which yield a dip of 80–85 degrees to the west.

Bodies within *Group 7* are constructed on the basis of airborne measurements alone. There is considerable uncertainty, but the shape of the magnetic anomaly indicates a dip towards the east.

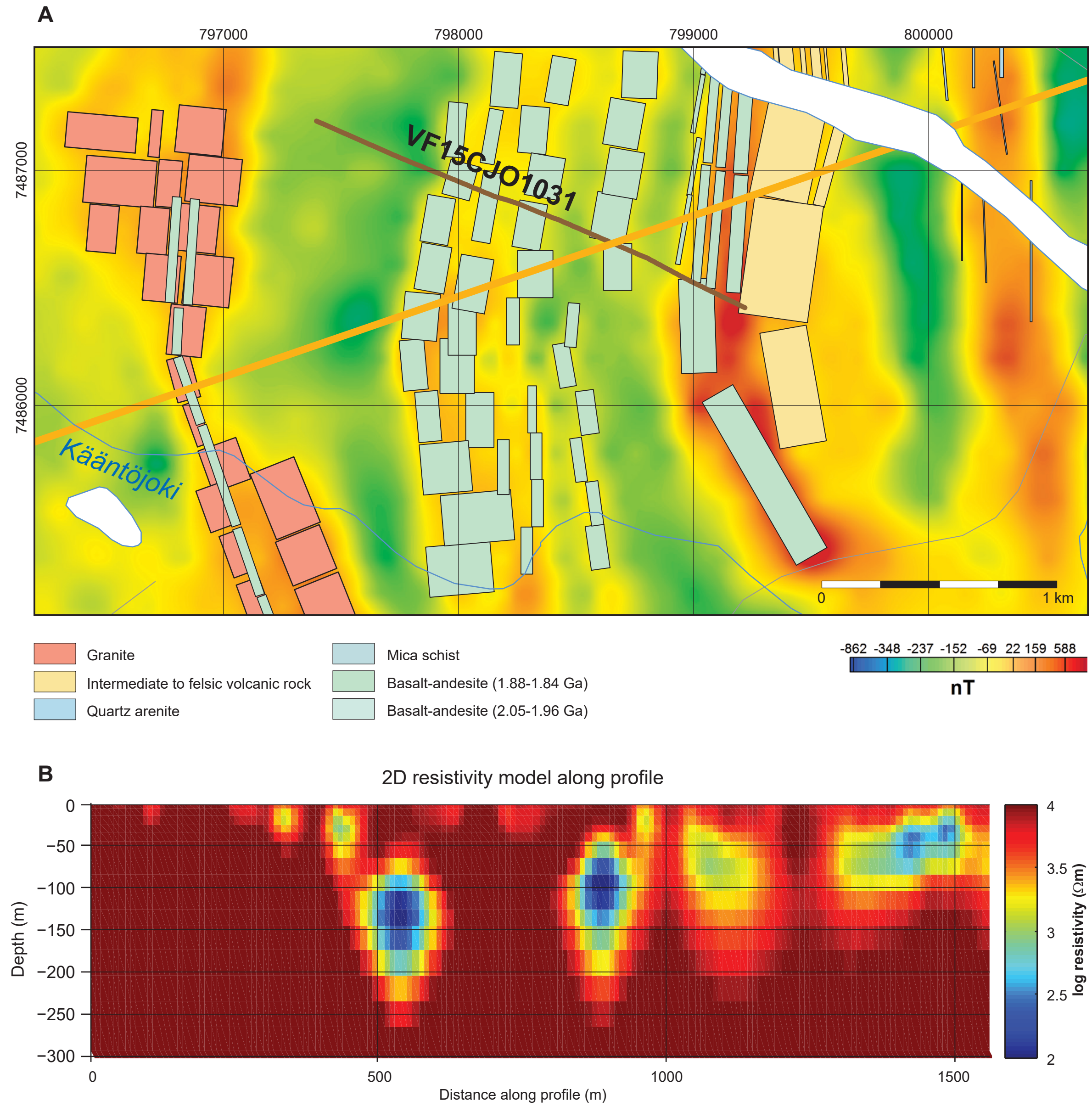

Figure 22. The location (A) and result (B) of the VLF profile "VF15CJO1031" in relation to modelled bodies. The resistivity cross-section shows the subsurface conditions down to 300 m below the ground surface.

Mica schist makes up *Groups 8, 9 and 11*, the lateral extent of which is covered by ground magnetic data. The bodies in *Group 8* have very low susceptibility, whereas the anomalies associated with *Group 9 and 11* are also clearly outlined in the airborne magnetic data. The bodies in *Group 9* are thin, 5–50 m, and are vertical or dip steeply towards the east. Figure 24C shows a sample of mica schist with a magnetic susceptibility of 0.03 SI. The bodies in *Group 9* are assumed to represent this rock. The bodies in *Group 11* are approximately 80 m wide and dip steeply towards the east (Fig. 25). No outcrops are present in the modelled area, but further north, along the same anomaly, there are numerous observations and sampling sites constraining the geometry and susceptibility values of the groups.

On the current bedrock map, a thin horizon of basic volcanic rock (Figs. 9 and 17a) is intercalated with the quartz arenite sedimentary package. This horizon has been assigned the name *Group 10* in the model. Observations and sampling show that this is a basaltic horizon approximately 10 m wide with a susceptibility of 0.02–0.03 SI and vertical dip. The basaltic horizon is altered and heterogeneous (Figs. 26A–C), locally banded at cm scale.

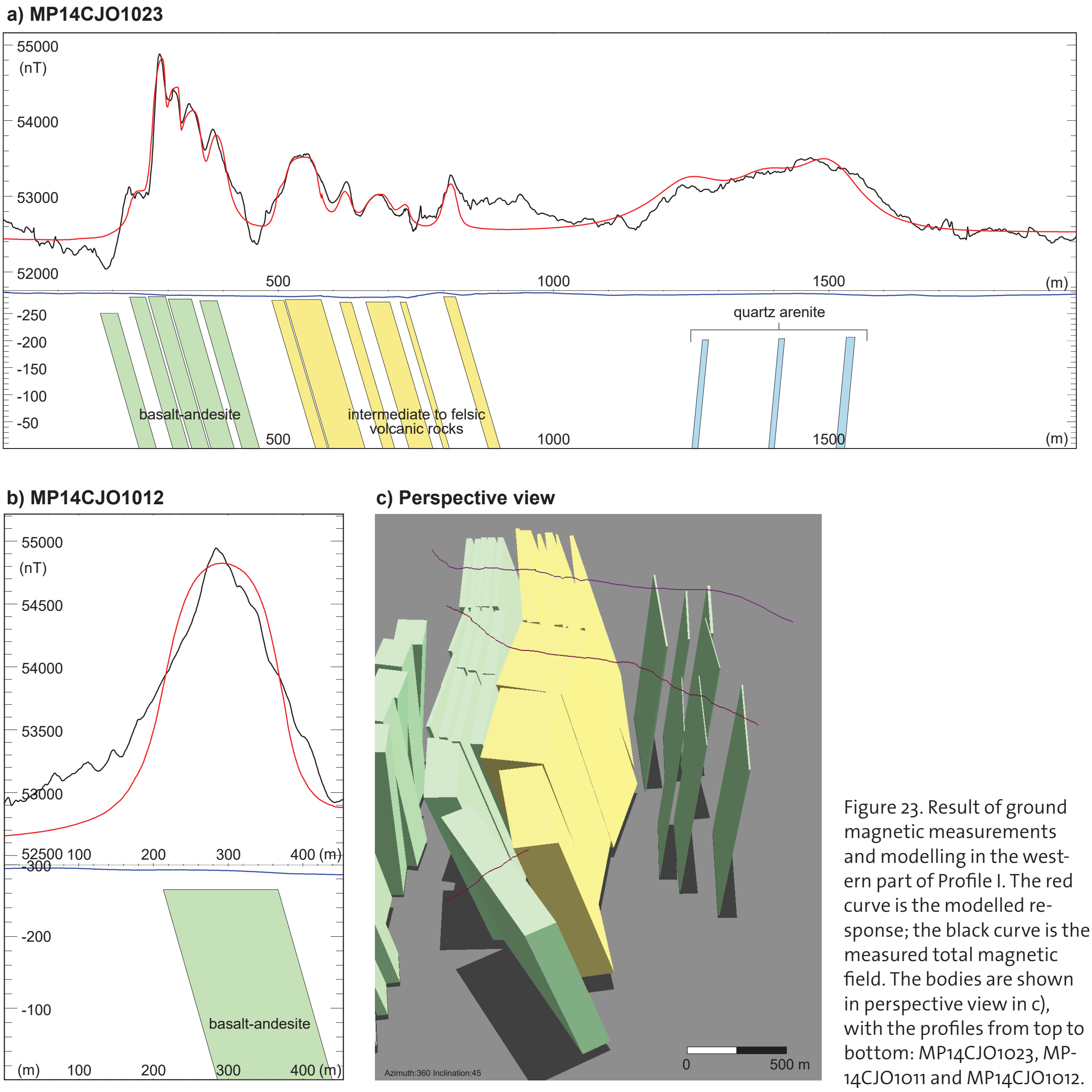

Figure 23. Result of ground magnetic measurements and modelling in the western part of Profile I. The red curve is the modelled response; the black curve is the measured total magnetic field. The bodies are shown in perspective view in c), with the profiles from top to bottom: MP14CJO1023, MP-14CJO1011 and MP14CJO1012.

Figure 24. **A**. Intermediate volcanic rock with a magnetic susceptibility of 0.03 SI. The light area of the rock is the weathered surface. (E 799311,N 7487739, ID: CJO141063).

C. Mica schist. (E 804543, N 7492262, ID: CJO141068). Coordinates in SWEREF99 TM.

B. Fine-layered arenite with highly variable magnetic susceptibility. (E 800130 N 7487177, ID: CJO141060).

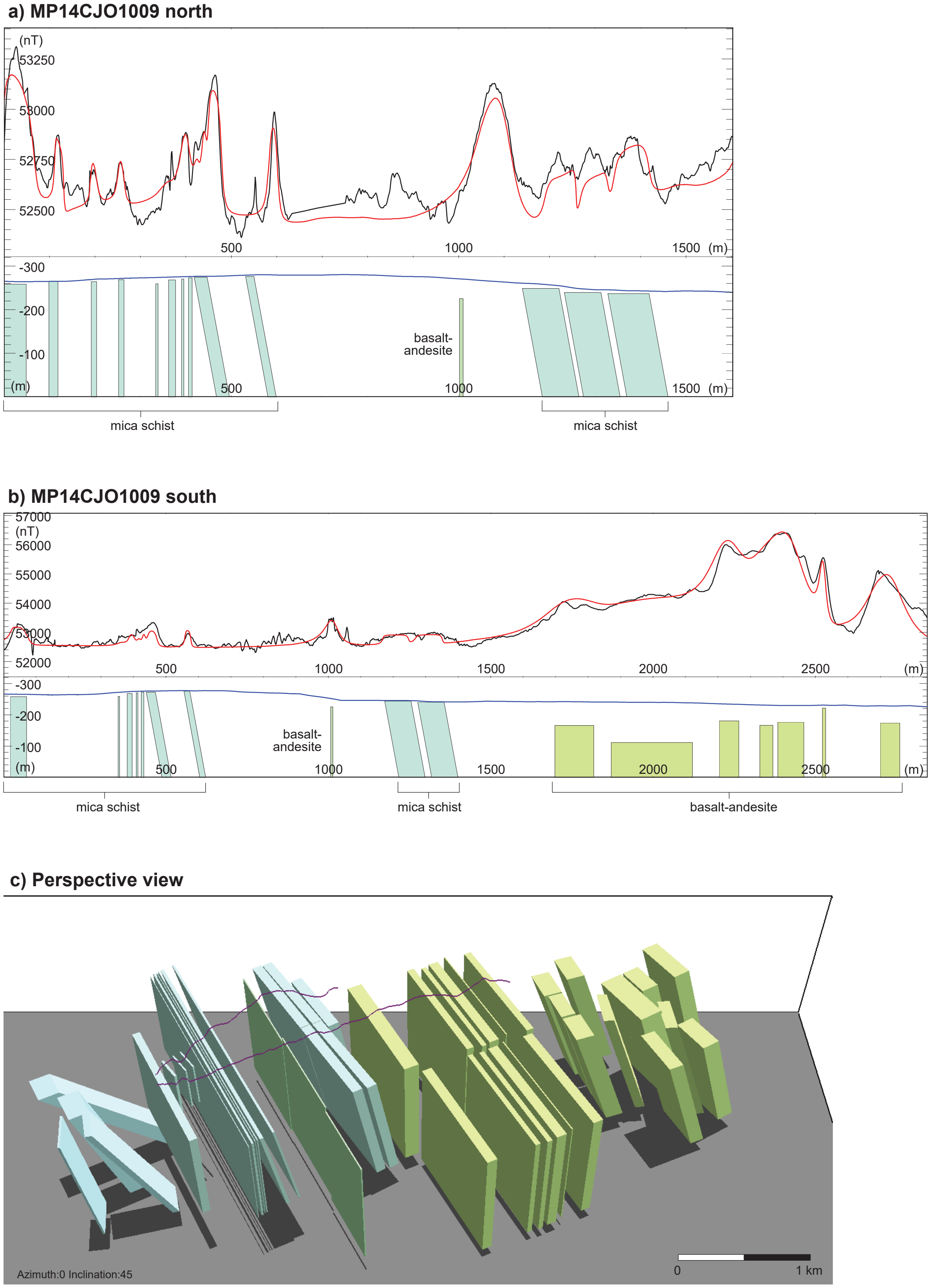

Figure 25. Results of ground magnetic measurements and modelling in the eastern part of Profile I. The red curve is the modelled response; the black curve is the measured total magnetic field. The bodies are shown in perspective view in c), with the profile MP14CJO1009, north and south parts.

Figure 26. A–C shows different appearances of the basaltic rock intercalated in a sedimentary rock unit. The samples were taken within 10 m of each other (SWEREF99 TM: E 806837, N 7489784. ID: CJO151073).

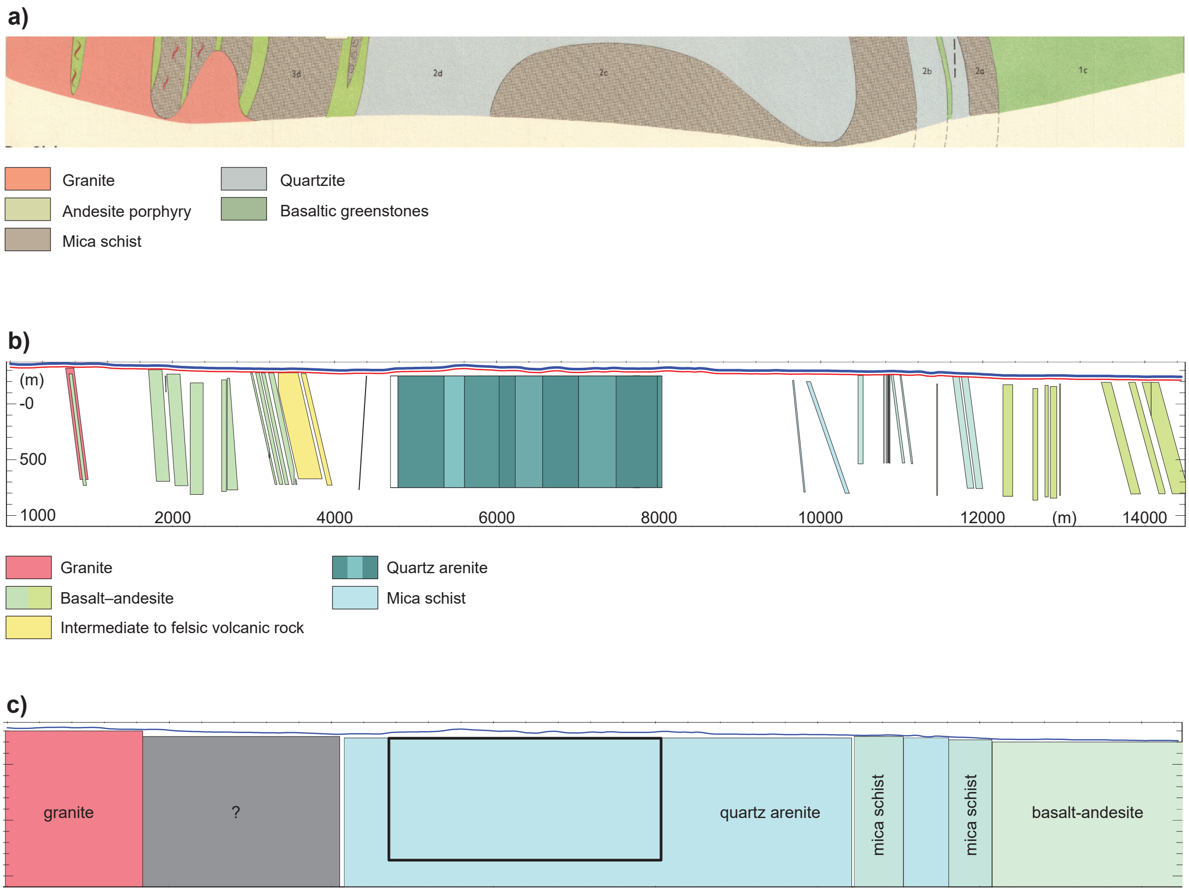

Figure 27. Comparison between the old (a) and new (b) models. c) shows the background bedrock type in the new model.

Groups 12 and 13 consist of the *Veikavaara greenstone group*, whose high magnetite content causes a high-magnetic pattern on a regional scale (Fig. 10) folded to a V shape in the southern part. These rocks cover an extensive area, but with few outcrops and thus observations and samples. *Group 12* is covered by ground magnetic measurements by profile MP14CJO1009 (Fig. 25) Observations and samples north of the profile in association with another ground magnetic profile have been used to increase the reliability of the model. This assumes that the rocks do not change much along the horizon on which they are found. The model gives upright horizons of varying width (10 to 120 m) for *Group 12* and easterly-dipping horizons for *Group 13*. Magnetic susceptibility is very high: between 0.1 and 0.3 SI.

CONCLUSION

The geological and the geophysical models generated in this study are compared with each other in Figure 27. The "background" bedrock types in the different areas are also included. The grey area in the western part of Figure 27c) is not named, since it is not certain whether it is mica schist, according to Padget (1970), or basic volcanic rock, according to Bergman et al (2001).

It is evident that several areas match between the two models but that there are also some discrepancies. The largest discrepancies between the models are found in the areas for *Groups 4 and 5*, basaltic and intermediate to felsic volcanic rocks. The new model shows that layers dip approximately 75 degrees towards the east, while the older model shows westward dips. An eastward dip is supported both by newly acquired ground magnetic data and by automated strike/dip calculations, so this is stated with confidence.

Another area where the structures differ occurs in the western part of the profile, but here there are far fewer structural indications to resolve the differences. In the eastern part of the profile, the old and new models show a similar character, but the new model resolves the different horizons to a higher degree. It also provides the link between the magnetic susceptibilities of the rocks and the magnetic anomalies observed.

REFERENCES

Bastani, M. & Pedersen, L. B., 2001: Automatic interpretation of magnetic dike parameters using the analytical signal technique, *Geophysics 66*, 551–561.

Bergman, S., Kübler, L. & Martinsson, O., 2001: Description of regional geological and geophysical maps of northern Norbotten County. *Sveriges geologiska undersökning Ba 56*, 110 pp.

Bergman, S., Stephens, M.B., Andersson, J., Kathol, B. & Bergman, T., 2012: Bedrock map of Sweden, 1:1 000 000 scale. *Sveriges geologiska undersökning K 423*.

Eriksson, B. & Hallgren, U., 1975: Description of the geological maps Vittangi NV, NO, SV, SO. *Sveriges geologiska undersökning Af 13–16*, 203 pp. (in Swedish with summary in English).

Grigull, S., Berggren, R., Jönberger, J., Jönsson, C., Hellström, F. & Luth, S., 2018: Folding observed in Palaeoproterozoic supracrustal rocks in northern Sweden. *In:* Bergman, S. (ed): Geology of the Northern Norrbotten ore province, northern Sweden. *Rapporter och Meddelanden 141,* Sveriges geologiska undersökning. This volume pp 205–257.

Hellström, F. & Jönsson, C., 2014: Barents project 2014, Summary of geological and geophysical information of the Masugnsbyn key area. *Sveriges geologiska undersökning SGU-rapport 2014:21,* 84 pp.

Hellström, F. & Jönsson, C., 2015: Summary of geological and geophysical field investigations in the Masugnsbyn key area, northern Norrbotten. *Sveriges geologiska undersökning 2015:04*, 31 pp.

Lynch, E.P. & Jönberger, J., 2013: Kartering Barents 2013, Summary report on the geological and geophysical characteristics of the Nunasvaara key area. *Sveriges geologiska undersökning SGU-rapport 2013:11,* 35 pp.

Lynch, E.P., Hellström, F.A., Huhma, H., Jönberger, J., Persson, P.-O. & Morris, G.A, 2018: Geology, lithostratigraphy and petrogenesis of c. 2.14 Ga greenstones in the Nunasvaara and Masugnsbyn areas, northernmost Sweden. *In:* Bergman, S. (ed): Geology of the Northern Norrbotten ore province, northern Sweden. *Rapporter och Meddelanden 141,* Sveriges geologiska undersökning. This volume pp 19–77.

Padget, P., 1970: Description of the geological maps Tärendö NW, NE, SW, SE with an appendix on geophysical aspects by J.D. Cornwell. *Sveriges geologiska undersökning Af 5–8*, 95 pp.

Witschard, F., Nylund, B. & Mannström, B., 1972: Masugnsbyn iron ore. Report concerning the results of Sveriges geologiska undersökning:s investigations in the years 1965–1970. *Sveriges geologiska undersökning BRAP 734,* 96 pp.

Geological Survey of Sweden
Box 670
SE-751 28 Uppsala
Phone: +46 18 17 90 00
Fax: +46 18 17 92 10
www.sgu.se

Uppsala 2018
ISSN 0349-2176
ISBN 978-91-7403-393-9
Tryck: Elanders Sverige AB